Aalto-yliopisto
Aalto-universitetet
Aalto University

Effects of elastic buckling at subcritical loads on the load carrying mechanism of a modern passenger ship

Alexander G. Jerne

Thesis submitted for examination for the degree of Master of Science in Technology

Espoo 20.02.2021
Supervisor: Professor Jani Romanoff, Aalto Yliopisto
Advisor: M.Sc. (Tech.) Oliver Parmasto, Foreship OY

Abstract

Author Alexander G. Jerne

Title of thesis Effects of elastic buckling at subcritical loads on the load carrying mechanism of a modern passenger ship

Master programme Mechanical Engineering **Code** ENG25

Thesis supervisor Professor Jani Romanoff

Thesis advisor(s) M.Sc. Oliver Parmasto

Date 20.02.2021 **Number of pages** 33 **Language** English

Abstract

This work assesses the effect of local elastic buckling on the load carrying mechanism of a modern passenger ship. A qualitative description of the effects the reduced stiffness of elastically buckled structures has on the passenger ship's load carrying mechanism is provided. The goal is to identify the scenarios in which the reduced stiffness of the load carrying structures must be accounted for. The identification is done through a global strength analysis of a passenger vessel using nonlinear finite element analysis, which better represents the stiffness deviations caused by load shedding in the elastic range, and to compare the results with those obtained from a classic linear static analysis.

The results show how the resulting nonlinearities can significantly alter the load carrying mechanisms at various structural hierarchy levels, even as load levels far below the ultimate limit state, and that simple linear static finite element solutions are unable to capture these effects.

The study differs from previous ones by investigating nonlinear effects on the hull girder at subcritical loads, instead of trying to find the ultimate strength when these nonlinearities are included. This work could be expanded in the future by reaching subcritical load levels closer to the ultimate limit state in order to capture greater global effects of these phenomena, or by implementing more efficient modelling techniques capable of greatly reducing the computational problem size.

Keywords Passenger Ship, Elastic Buckling, Nonlinear Analysis, Finite Element Method, Load Carrying Mechanisms

Acknowledgements

Foreship Ltd. generously financed this study, provided me with a supportive workspace and the tools necessary to carry out my work; a heartfelt thank you is due.

I would also like to thank both my advisor Oliver (M.Sc. Tech.), for going far beyond his due duties in order to help my produce something I am proud of, and my supervisor professor Jani Romanoff (D.Sc. Tech.), for his guidance and trust, mostly expressed through the freedom to work at my own pace which was granted me.

The completion of this thesis seals a chapter of my life which I will be eternally grateful to have had the opportunity of experiencing. I believe I will always look back at this adventure, spent mostly in quiet Espoo and on-board crowded Tallinn-Helsinki ferries, with sincere fondness. The challenges and difficulties encountered throughout this time were faced head on and gladly, which made it easier for them to be overcome. This was possible thanks to the fine company of people who filled my days in Finland with happiness and camaraderie, while also setting high standards for me to strive towards. Thank you, friends. Finally, I would also like to express my gratitude to Liisa, who's patience, courage and understanding were the great invisible pillar sustaining it all.

Tallinn, 11.02.2021

Alexander G. Jerne

Table of contents

1. Introduction

1.1. Background

As consumer demand (see Figure 1) and competition in the cruise ship market surge, the increasingly large newbuilds require the utilization of innovative lightweight solutions in order to improve energy efficiency through weight reduction, by means of using ever thinner plates made of high strength steels. The required thin and slender structures are often likely to have initial distortions which cause nonlinearity in both global and local structural responses which are still in the process of being fully understood and require further investigation (Romanoff et al., 2020).

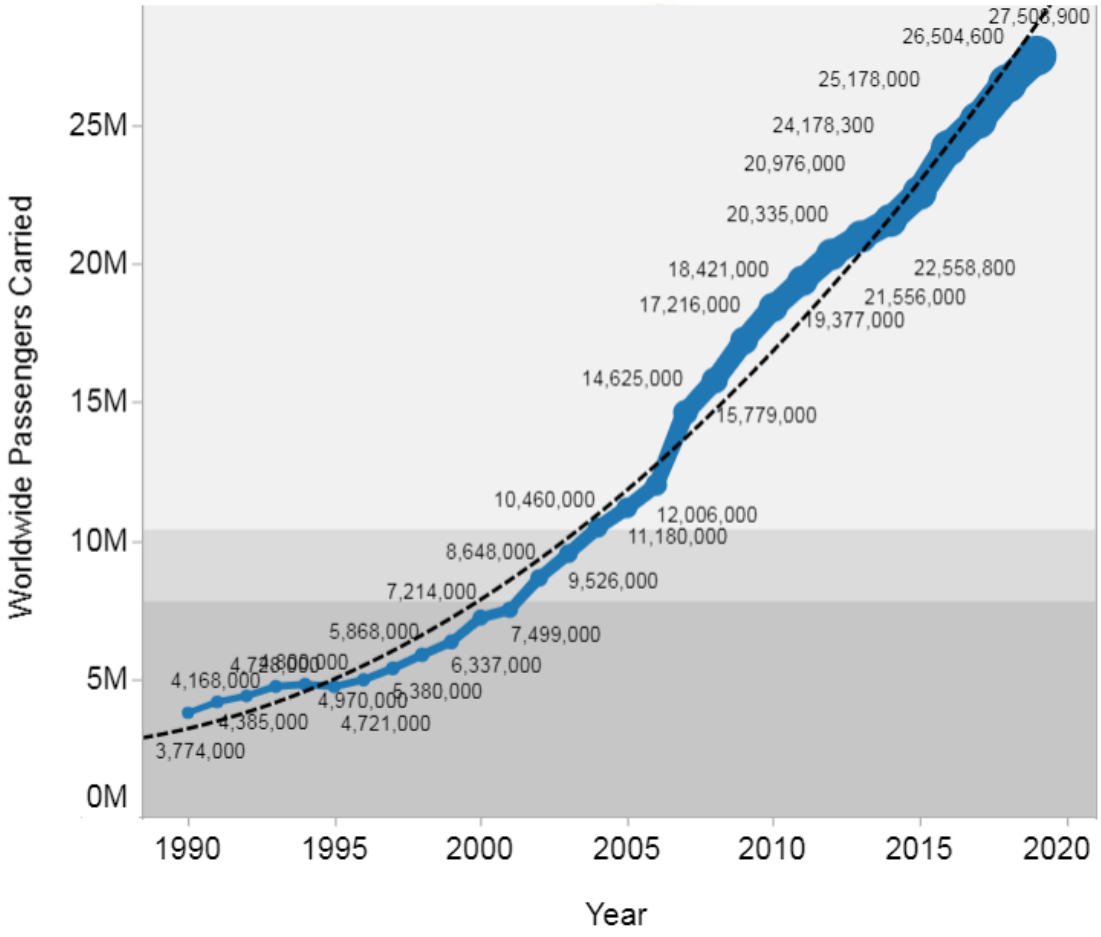

Figure 1. Growth in worldwide passengers carried by the cruise industry from 19990 until pre COVID-19 pandemic peak in 2020 (©Cruise market watch, 2021).

This holds especially true when faced with the onset of modern Ultimate Limit State (ULS) design principles, where ultimate capacity has become the defining limit, in contrast to elastic buckling, as was seen in the past (DNVGL, 2015). Most standard design formulation for plated structures have been developed based on linear plate buckling theory. The time in which the highly appreciated hand-calculation and explicit formulation methods, aided by empirical correction factors, were the most sophisticated tools available, has come to an end (Palm, 2015). Computerized tools are increasingly becoming accepted and ship owners and yards are keener than ever to carefully search for any advantage, in form of cost saving, performance improvement and not less importantly,

branding. Having the lightest, most efficient structure, while also catering to the modern passengers' increasingly environmentally conscious driven demands, could very well be the deciding factor will give them the edge on the competition and move their business ahead of the curve.

Generally, in a ship's structure, the elastic buckling of stiffened plate panels is not considered critical as notable post buckling strength carrying capacity still exists when enough support at the edges of the plates is provided (DNVGL, 2015). However, thin plate structures will lose some of their stiffness in case of elastic buckling of plates due to load shedding, which occurs in the post buckling range. In a complex modern passenger ship structure, this will lead to the redistribution of global loads over the entire ship cross-section and may induce secondary effects which will not be captured with linear finite element analysis, or which require time-consuming nonlinear analysis methods, ill-suited for the crucial initial design stages (Steen, E. et al., 2008; Melk, 2011; Parmasto, 2012; Palm, 2016). Being that stiffened panels make up significant portions of the structure, the need arises for more sophisticated design procedures that cope with all relevant non-linear effects, and are simple enough to compete with established methods.

1.2. State of the art

Amongst the primary requirements for any marine structure, it is fundamental for them to be safe, not have catastrophic failure nor incur in operational difficulties due to modes of failure. The analysis of the structure and design procedure involve determining design loads, acceptable criteria definition and strength assessment. Once the loads and acceptance criteria are defined, the strength assessment is carried out, during which the load distribution must be determined (Shama, 2013).

For the design of passenger vessels in particular, due to the nature of their cargo, structural characteristics and the high incentive to reduce weight, understanding load distribution plays a paramount role. Principles derived from Euler-Bernoulli beam theory, traditionally used in ship building to understand structures and their responses, proved to be ineffective for the superstructure of passenger vessels and even more so its interaction with the hull girder. This is mostly due to the incremental size of deckhouses and the resulting increase in contribution on the overall global strength. Vasta's model scale tests in the late 40s made this clear, showing that longitudinal strains were nonlinearly distributed in the mid-ship section, indicating a significant break at the "promenade deck". This finding goes against Navier's hypothesis that the plane sections remain plane at bending (Vasta, 1949).

The following decade saw various efforts to generate theoretical models capable of describing the phenomenon observed during Vasta's experiments. Crawford hypothesized that the strain distribution nonlinearities are caused by the different cross sections of the hull and deckhouse, but that beam theory was still applicable to the hull and deckhouse individually (Crawford, 1950). It was only a couple of years later than Bleich formulated a model in which both hull and deckhouse behave as two separate beams which act together by transferring shear forces and with vertical forces resisting relative displacement. His method neglects shear lag effect and considers the superstructure (in the form of a deckhouse) as an elastically supported beam on the hull, attached to the hull at the deck level in a manner which enforces equal strains at the connection points (Bleich, 1952). Caldwell builds on this, revealing the effects the deckhouse has on the longitudinal strength

of the hull and formulating a method for determining stress distributions due to the bending moments a ship is subjected too. Large side openings are still being neglected at this point (Caldwell, 1957).

It was in the 60s, due to the increase in demand for transoceanic voyages and a boom of the cruise industry, that passenger vessels began to drastically change (see Figure 2). Deckhouses start being replaced by broad superstructures with multiple thin deck. These new superstructures had large openings to accommodate new needs, which substantially complicated the load carrying mechanisms; these new structures required further study and understanding. Less than a decade later, Caldwell continued his previous work through the development of a method to calculate the ultimate longitudinal strength of a ship (i.e. highest bending moment the structure can withstand), including a reduction in this strength due to buckling of decks. The buckling strength depends not only on the sectional properties of the stiffening elements and the effective width of the plating acting on said stiffeners, but also on the spacing of the supporting transverse frames (Caldwell, 1967). As the demand for larger and increasingly complex superstructures rose, so did the necessity for increasingly light structures, which in turn introduced even more stiffness related issues. It had become clear that a serious obstacle to accurately determine ultimate hull strength has been the lack of understanding regarding the effects of local buckling of stiffened panels, which experience compressive loads in passenger ships.

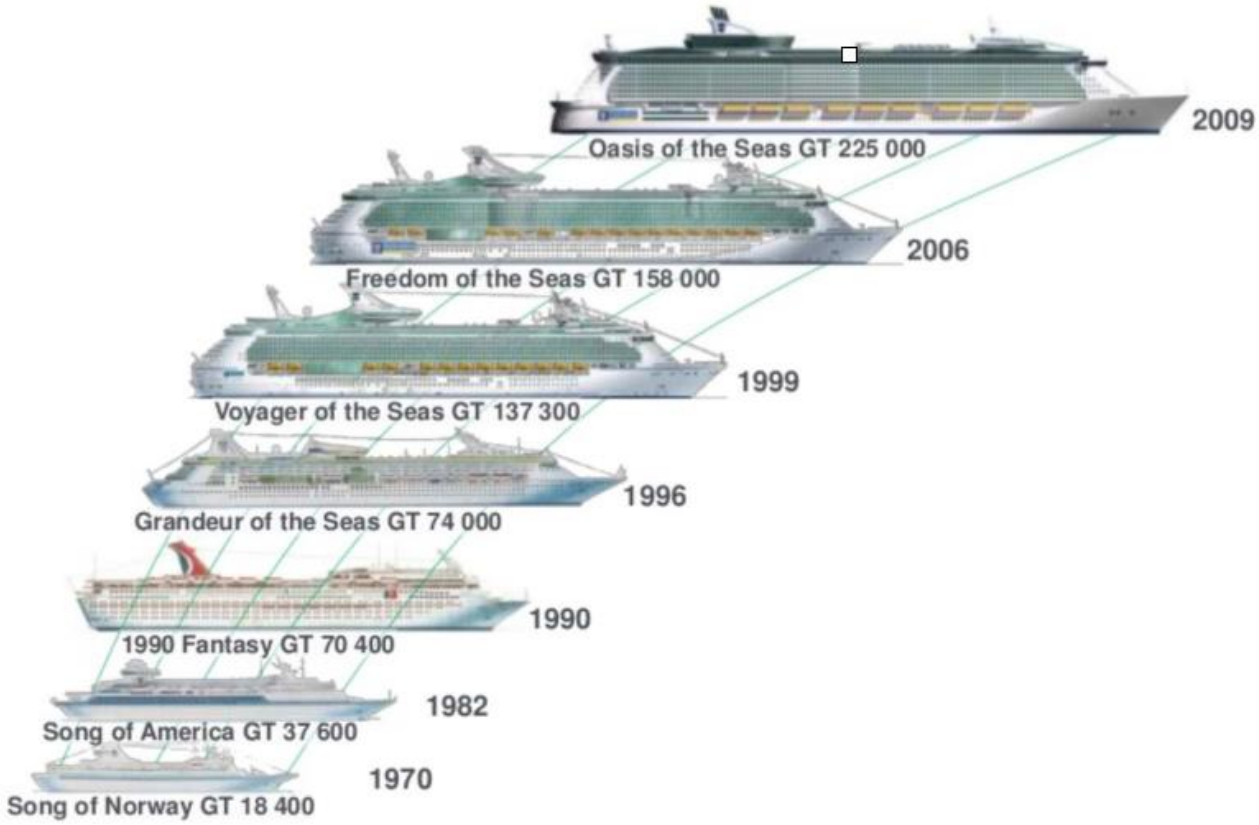

Figure 2. Gradual increase in size and complexity of the cruise ship from 1970-2010; (STX Europe/Mayer Turku, 2018).

As in other fields on engineering, eventually the finite element method (FEM) gained foothold in shipbuilding for various types of structural analyses. Heder and Ulfvarson, in the early 90s, presented a simplified method for evaluating the global behaviour of the hull and superstructure. The method was based on a 2D FE-model for evaluating bending stress distributions for ships with large stiffness reducing openings arbitrarily located over the flat side shell, typical of modern passenger vessels (Heder and Ulfvarson, 1991). Their method didn't account for the effect of shear lag though, caused by hull-superstructure interaction.

In order to make the FEM more desirable at initial stages of design, the optimisation of structures and meshing techniques in concept design stage began being further investigated. One of these methods comprised of initial evaluation of the cruise ship structure with 3D FEM in order to obtain the normal strain distribution. The optimisation is conducted on a 2D section, assuming that the normal strains will be distributed similarly in the different designs (Andric & Zanich, 2010). At the same time, as the models grew more complex and the computational time increased exponentially, efforts were made to improve previous swifter beam theory-based methods to apply to new structures, using the FEM as a validation tool.

An example of this is the work carried out by Naar in the early 2000s, who advocated a Coupled Beam (CB) method, modelling each deck, in both superstructure and hull, as individual think-walled beams, coupled by springs. In this method, using calculated normal stresses and vertical deflection, it is possible to estimate the shear stresses in the side structures. The study captured nonlinear behaviour in the form of elastic plate buckling at subcritical load levels. As shown in Figure 3, both the side shell of the recess ares at x=3L/4 and the top deck at midship buckle elastically, without affecting the overall structural stiffness of the hull girder. This work was validated using a three-dimensional finite element analysis (Naar et al, 2004; Naar, 2006).

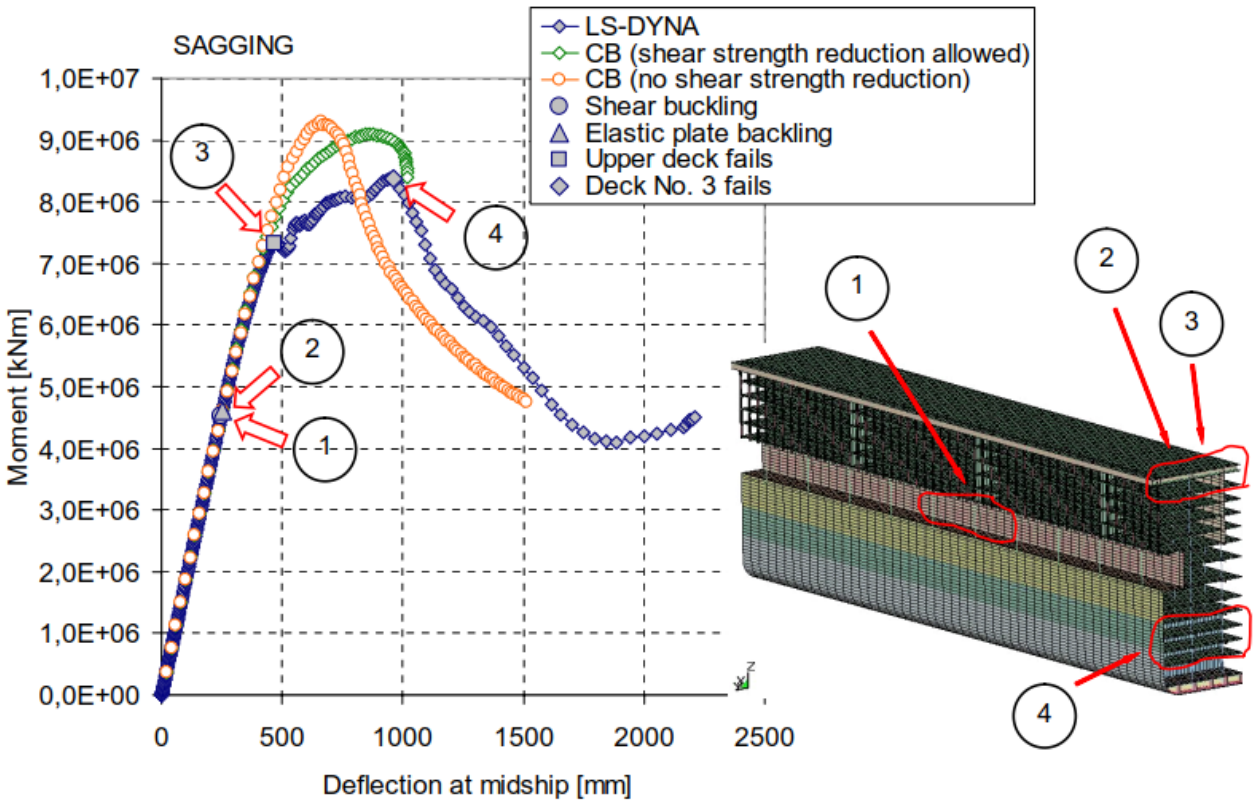

Figure 3. Moment-Deflection curve under sagging condition (Naar, 2006).

Naar's work focused on validating his simplified method for accurately determining the ultimate strength of passenger ships and capturing realistic structural failure mechanisms, which also accounted for nonlinearities. Understanding failure modes and load carrying mechanisms were not the priority. However, nonlinear behaviours with a potential to have global structural effects require further in-depth study, in order to fulfil both the current serviceability limit states (SLS) and ULS.

Authors like Lillemäe and more recently Ekman, have shed a brighter light on how structural loads redistribute on local level to tertiary and secondary elements at the onset of elastic buckling. Once buckled, deck plates lose stiffness and this causes their primary and secondary stiffeners to be subjected to higher load levels, rendering them more efficient (Lillemäe et al., 2013 & 2014; Ekman, 2020). The effects this has on a global level, however, remains yet to be assessed. This is especially the case for passenger ships. whose failure modes are particularly difficult to predict, due to the complex structural behaviour. Parmasto's findings provide a great example of how hull-superstructure interaction induce secondary effects in these large vessels (Parmasto, 2012).

1.3. Purpose and scope

The aim of the thesis is to assess the effect of elastic buckling of plates on the load carrying mechanism of a modern passenger ship structural concept. A qualitative description of the effect of the reduced stiffness of elastically buckled structures on the passenger ship load carrying mechanism will be provided. The goal is to identify a scenario in which the reduced stiffness of the load carrying structures must be accounted for in a modern passenger ship. The identification will be done through a global strength analysis of a passenger vessel using nonlinear finite element analysis, which better represents the stiffness deviations caused by load shedding in the elastic range, and to compare the results with those obtained from a classic approach, using a linear static analysis.

2. Methods

2.1. Global strength calculation methods for passenger ships

A great number of methods have been proposed for evaluating the response of passenger ships, most of which were developed before the digital age and are therefore based on classic strength of material, beam theory and/or plane stress theory. Already in the early 50s, Bleich had demonstrated how the various classical beam theories were inapplicable for studying passenger vessels with large deckhouses. Their incapability of capturing shear effects resulting from the connection between the deckhouse and hull, such as that of shear lag in the main deck or in the deckhouse sides, made them unsuitable (Bleich, 1952). This became even more relevant as deckhouses were replaced by superstructures. More suitable beam theory-based methods for describing global behaviour of modern passenger vessels emerged in the following decades, most notably the ones by Muckle and later by Naar et al. with the Coupled Beam method. They both take into account the influence of large side openings on the efficiency of superstructures, which allowed to capture some of the shear effects in multideck structures and their sides, while successfully reproducing the vertical stiffness of the main deck (Muckle, 1962; Naar et al., 2004). However, neither of the methods can account for the effects of shear lag in the main deck and its subsequent effect on the shear flow, which in turn plays a key role in determining the overall stiffness behaviour of the modern passenger vessel. The importance of taking these effects into account can be seen in the work done by Lillemäe (Lillemäe et al., 2013).

The superstructure essentially behaves as an elastically supported beam, with forces acting both in vertical and longitudinal directions, opposing their relative displacements, which are pointing in opposite directions at their connection (Bleich, 1952; Caldwell, 1957). Consequently, the resulting longitudinal shear forces at the connection between hull and superstructure will generate a moment resisting the moment of the superstructure. This mechanism is illustrated in Figure 4.

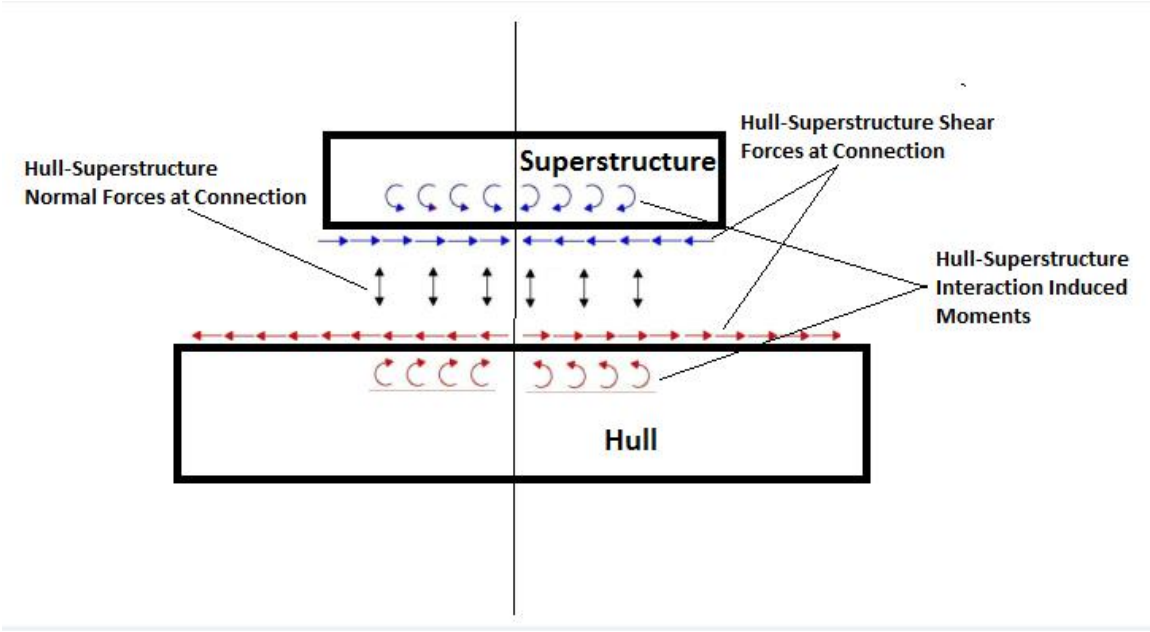

Figure 4. Deformed shapes and vertical forces.

This means that when the vessel is subjected to sagging, the superstructure will tend to rise outwards of the main hull at midship, while at the connection between the two, strong vertical forces will oppose this displacement. Meanwhile, it is important to keep in mind that at mid-ship, the applied pressure load is pointing in a negative direction, acting perpendicularly to the double bottom outer shell. At midship, this entails that at the cross-section the hull is being pulled downwards from its bottom shell, while also being pushed upwards at the connection to the superstructure, as shown in Figure 5. The decks of the hull will therefore be subjected to strong compressive forces in the transverse direction, causing the plates to buckle transversely to their stiffeners, in a plate driven buckling mode.

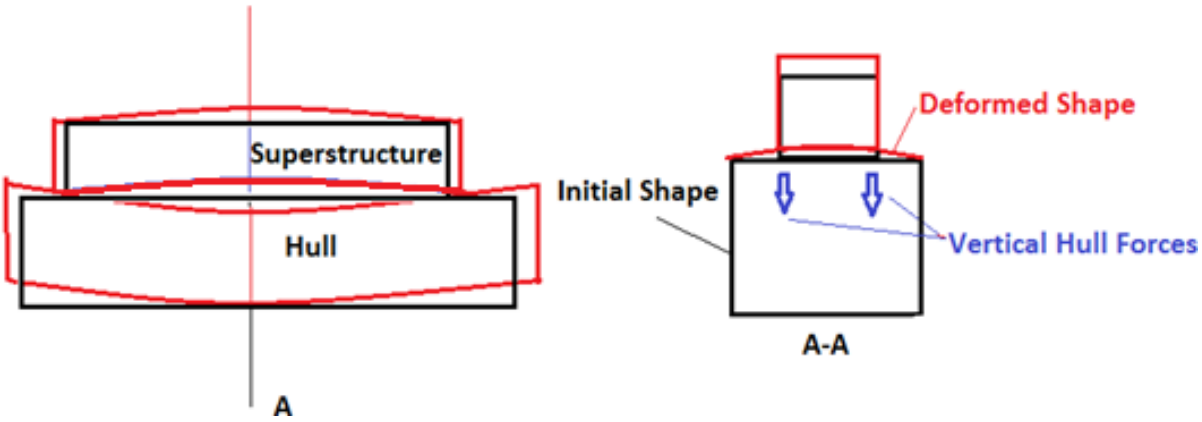

Figure 5. Forces and moments at superstructure-hull connection.

In terms of methods for global strength analyses, beam theory is still a more than valid option when carrying out this sort of evaluation for vessels such as modern bulk carriers. They lack both the disconnected unison between the hull and a superstructure which causes many of the secondary effects, and the presence of relatively thin, elastic buckling prone, stiffened panels normally present in the superstructures of large passenger vessels.

Amongst the most notable plane stress theory-based methods is the one by Caldwell, which was then built upon by both himself and other authors. This has briefly already discussed in the section regarding the stated of the art (Caldwell, 1957; Caldwell, 1967). These methods built upon plane stress theory, while having the advantage of taking into account most of the shear in hull and superstructure, are uncapable of dealing with multi-deck superstructure and are considered impractical and demanding to implement in a design (Parmasto, 2012). It is worth mentioning, that some of the analytical approaches mentioned up until this point, have been re-adapted for computer implementation, enabling their use at initial design phases.

Thanks to the advances of the computing capacity of computers during the past few decades, in tandem with significant software developments, three-dimensional FEMs have become a viable go to tool for studying structures such as that of the modern cruise ship. For the time being, FEAs are widely acknowledged as the most reliable mean for carrying out the type of investigation carried out in this thesis (ISSC, 1997). Moreover, simplified two-dimensional FE approaches such as that proposed by Heder & Ulfvarson, are usable at early design stages (Heder & Ulfvarson, 1991).

With regard to the use of FEM for passenger ships, due to the fact that it has become a widespread practice, the various classification societies offer guidelines for carrying out global strength

analyses. Generally applicable guidelines are also available for nonlinear studies and include descriptions of modelling techniques. The efficacy of these suggested methods and meshing techniques have been tested in studies such as those done by Naar and Parmasto (Naar, 2006; Parmasto, 2012). In this work, the methods employed will closely resemble those used in the abovementioned studies. This will allow for better comparison with other previously carried studies in which the reference model has already been analysed using comparable methodologies.

2.2. The finite element method

When using the finite element method, the calculation domain is divided into a finite number of elements connected by nodal points, also known as nodes. The original domain is in this way converted into a collection of pieces. The desired studied quantity is then solved for each individual node, the collective results of which being in turn interpolated over the elements they delimit, over the entire calculation domain. This interpolation within the element is carried out based on shape functions which are usually polynomials. Each element has different assigned properties selected in accordance to the nature of the problem and boundary conditions (Cook, 2001). For structural mechanics, a typical way of formulating the finite elements is using nodal displacements as the unknown for which to solve the system.

In order to find the solution to a linear static FE-problem, the following linear matrix equation must be solved:

$$\boldsymbol{Ku} = \boldsymbol{f}. \tag{1}$$

K being the structure's stiffness matrix, **u** the displacement vector and the external force vector being represented by $\boldsymbol{f}$. The load and displacements will increase at the same rate, due to the linearity of the equation and the superposition principles being considered valid (Kim, 2014). This is due to the stiffness being linear. Furthermore, due to the assumption that the displacements are infinitesimally small, the equilibrium equation can be solved in the undeformed initial condition, which justifies the use of the term "static". These assumptions are not considered to be valid in nonlinear analyses, now requiring the equilibrium equation to be solved incrementally as the shape is deformed, since neither the stiffness nor the external force vector are longer constant. Geometric nonlinearity, kinematic nonlinearity, material nonlinearity, following forces or a combination of any of these are possible origins of nonlinearity in a structural analysis. The geometrical and material nonlinearities cause **K** to no longer increase linearly, while kinematic ones are responsible for the shift in the behaviour of $\boldsymbol{f}$.

Due to this increase in complexity, nonlinear analyses generally require noticeably more time to be solved when compared to linear ones. Limiting the sources of nonlinearity to only a select most meaningful ones, unable of being captured by a linear analysis, is therefore important. Different nonlinear problems vary in degrees of nonlinearity. A material having a bilinear elastic-plastic behaviour, such as that of an elastically buckled deck at subcritical loads, will exhibit a behaviour far less nonlinear than those present in a complex contact problem, in which the boundary conditions vary greatly as each step progresses, as would be the case when an ultimate strength scenario is reached. The selection of increment sizes and stiffness matrix update strategies should be made keeping the factors in mind.

The system of nonlinear equations takes the following form:

$$\boldsymbol{P}(\boldsymbol{u}) = \boldsymbol{f} \tag{2}$$

Where $\boldsymbol{P(u)}$ is the internal force vector and $\boldsymbol{f}$ the external forces, which is known. The displacement $\boldsymbol{u}$ is the unknown for which the equation is being solved. At each subsequent step, the stiffness calculated from the previous solution is used. Due to the presence of large displacements, when geometric nonlinearity occurs, the relation between strains and displacements in no longer linear. A great example of this is the occurrence of buckling, during which the induced geometric nonlinearity causes the elements to deflect more with the same increase in force as before buckling. On the other hand, material nonlinearity causes nonlinearities between strains and stresses. This type of nonlinearity can be caused by hyperplastic behaviour, such as that exhibited by rubber or some plastics.

In order for nonlinear problems to be solved, they are divided into smaller subsections, which in turn are linearized and solved individually. The smaller the change in load, the easier it is for the problem to be solved. Therefore, dividing the force into smaller increments is the first step. Next, through the use of suitable iteration methods, each increment of the problem is solved. The subsequent increment uses the previous solution as a guess from which to begin the next step. A widely used iteration method used for finding solutions to nonlinear equations, is the Newton-Raphson one, as shown by Kim in equation (18) (Kim, 2014). An initial estimate (u_0) is used to find and increment (Δu), so that their sum ($u_0 + \Delta u$) accurately represents a solution. The solution for the subsequent step/iteration can then be solved using a first-order Taylor series with the following formula:

$$\boldsymbol{P}\left(\boldsymbol{u}^{i+1}\right) \approx \boldsymbol{P}\left(\boldsymbol{u}^{i}\right) + \boldsymbol{K}_T^i\left(\boldsymbol{u}^{i}\right)\Delta\boldsymbol{u}^{i} = \boldsymbol{f}. \tag{3}$$

in which $\mathbf{K^i_T(u^i)}$ represents the tangent stiffness matrix. This equation can be rearranged to form the following:

$$\boldsymbol{K}_T^i\Delta\boldsymbol{u}^{i} = \boldsymbol{f} - \boldsymbol{P}\left(\boldsymbol{u}^{i}\right). \tag{4}$$

which represents a linear matrix equation solved for Δu, which when obtained, gives a new approximate solution of:

$$\boldsymbol{u}^{i+1} = \boldsymbol{u}^{i} + \Delta\boldsymbol{u}^{i}. \tag{5}$$

This solution being an approximation, it is possible to calculate the residual forces using this formula:

$$R^{i+1} = \boldsymbol{f} - \boldsymbol{P}\left(\boldsymbol{u}^{i+1}\right). \tag{6}$$

Once the residual force is found to be smaller than the given tolerance, the iteration sequence will stop.

Considering the scope of the study, the Newton-Raphson method is suitable and will be used. This method is sensitive to the modelling techniques used in the analysis. As the effects of elastic buckling are the focus of the study, the buckling modes must to be captured for the stiffness and force matrices to be subject to change. The meshing will play an important role to this regard. A mesh too coarse is unable to capture this behaviour, therefore there would be no difference in results whether a nonlinear or linear static model were used.

Figure 6 shows how the modified Newton-Raphson method differs from the original Newton method by updating the stiffness matrix only at the increment's first iterations. This is meant to significantly decrease computational times, the stiffness matrix computation being the "heaviest" process, computationally speaking, of the nonlinear analysis. There are also hybrid strategies, which combine the modified and original Newton-Raphson methods and update the stiffness matrix only a few iterations if the convergence is not reached (Ekman, 2020).

Once the structure reaches its limit point and collapses, the tangent stiffness matrix becomes singular and the Newton-Raphson methods are unable to predict structural response (Reddy, 2004; Ekman, 2020). At this point, in order to track solutions beyond the limit state, other methods can be utilized. The Riks, Modified Riks, or the Arc-length methods amongst them (Riks, 1979; Reddy, 2004; Steen et al., 2008). These methods are better suited for studying ultimate strength and post limit state scenarios.

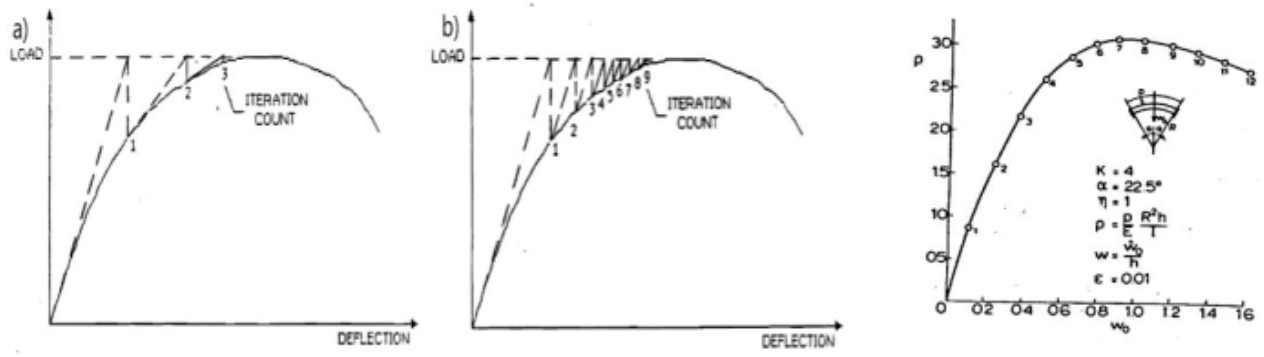

Figure 6. LEFT: Newton-Raphson method; CENTER: Modified Newton-Raphson method (Siemens, 2019); RIGHT: Riks method (Riks, 1979).

2.3. Finite element modelling techniques for passenger ships

2.3.1. Structural discretisation and FE mesh

The main objective of the global finite element model of a passenger vessel is to represent the global stiffness to a satisfactory degree, as the purpose of the analysis is to calculate the nominal stresses caused in primary members correctly. Another primary goal is the identification of possible critical areas of the structure to investigate in further depth and providing correct boundary conditions for eventual local analyses.

This, in turn, will allow for the secondary effects caused by the global loads to be "revealed". The vertical sinking of the decks, eventual shear lag, pillar bending and significant "S shaped" distortions of the external frames where large openings are present, all represent secondary effects caused by global loads. A useful example of these effects and how they can be studied is shown in the work done by Melk, which investigated the shear-induced bending responses at large balcony openings in passenger ships (Melk, 2011). Correctly capturing these phenomena is of vital

importance for modern passenger ships, as they play a significant role not only in determining fatigue life, but also in understanding the load-carrying mechanisms of the global structure.

Ideally, it is preferable to not need to model all structural elements present individually, as it adds complexity and computational requirements. The level of detail of the model is dependent on its complexity and size. A significant portion of the ship's structures it made up of stiffened panels and other stiffening structural elements such as girders and web frames. Stiffening elements are classified into primary, secondary and tertiary categories. Modelling primary ones (i.e. girders and web frames) is necessary due to the direct influence the play on the response of the structure, and this is usually done using either shell or membrane elements (Shama, 2013).

Secondary stiffeners (i.e. plates and their stiffeners) can be modelled in various ways. The work done by Reddy and more recently Benson et al., provide great examples of the application of the equivalent single later theory (ESL), by attributing the properties of several layers of structures to a single layer element (Reddy*, 2004; Benson, 2014). Other developments followed suit, with focus on the interaction of these new structural elements and the rest of the vessel (Romanoff et al., 2011; Romanoff et al., 2016). A possible approach is to model the entire stiffened panel as a single laminate element with equivalent stiffness, homogenizing the combined behaviour of its structural elements (i.e. plate, stiffener web and flange) into a single element, as shown in Avi's work (Avi et al., 2015). Avi et al. extended the ESL theory for stiffened panel, where it is described as a three-layered laminate element. The first layer represents the plate, second layer represents the stiffener web and the third layer represents the stiffener flange. The element enables to change the parameters of secondary stiffeners such as type and spacing directly from the orthotropic material properties, without re-meshing the model. This allows the optimisation of wide range of materials and geometrical configurations (e.g. stiffened panels, laminates and sandwich panels) (Avi et al., 2015). Also, for the secondary stiffeners, the offset beam concept, which was applied in Ehler's work, can be applied. Here, the web of the stiffener is modelled as a shell element and the flange as a beam element at the shell's edge. The webs are modelled using quadrangular elements, while the flanges are modelled by using two node beam elements. An illustration of this technique is presented in Figure 7. When this technique is used, the moment of inertia and the combined area of the elements must be equivalent to that of modelled stiffeners. In many cases though, this level of detail doesn't represent a viable solution.

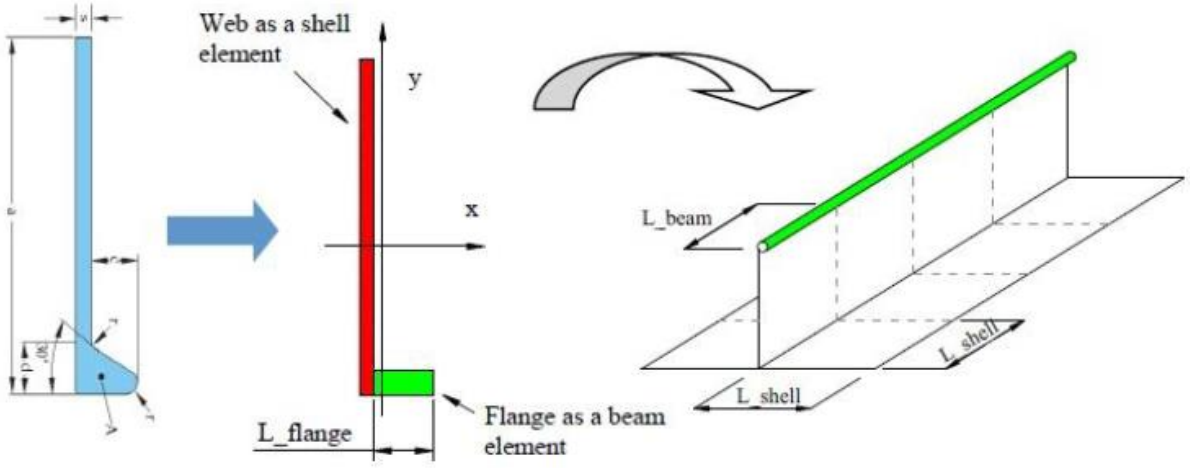

Figure 7. Offset beam technique concept visualized (Ehlers, 2011).

Large openings and pillars should always be included in the model, which can be done explicitly or by using homogenized coarse mesh elements. The bilge represents the principle curved structural element in the ship's hull. Using at least a pair of plate elements at the turn of the bilge is considered sufficient by most classification societies (DNVGL, 2018).

Naar had observed that in order to simulate proper collapse and capture nonlinear behaviour of stiffened deck panels, at least four shell elements between each stiffener have to be used and that the longitudinals can be modelled using a single shell element for the web and another for the beam, with offset (Naar, 2006). This is less strict than the classification society guidelines issued a year later, but was proven to be sufficient in Naar's dissertation in which a comparison was made to extremely fine meshes of two types, as seen in Figure 8. It is important to note though, that Naar had exclusively focused on stiffened plate models subjected to axial compression to derive the curves seen in Figure 8, which might limit the ability to capture curvature in order directions (DNVGL, 2007; Naar, 2006). A meshing technique somewhat similar to this will be the one used here, as the it proved successful for a comparable ship structure and will allow for a good comparison.

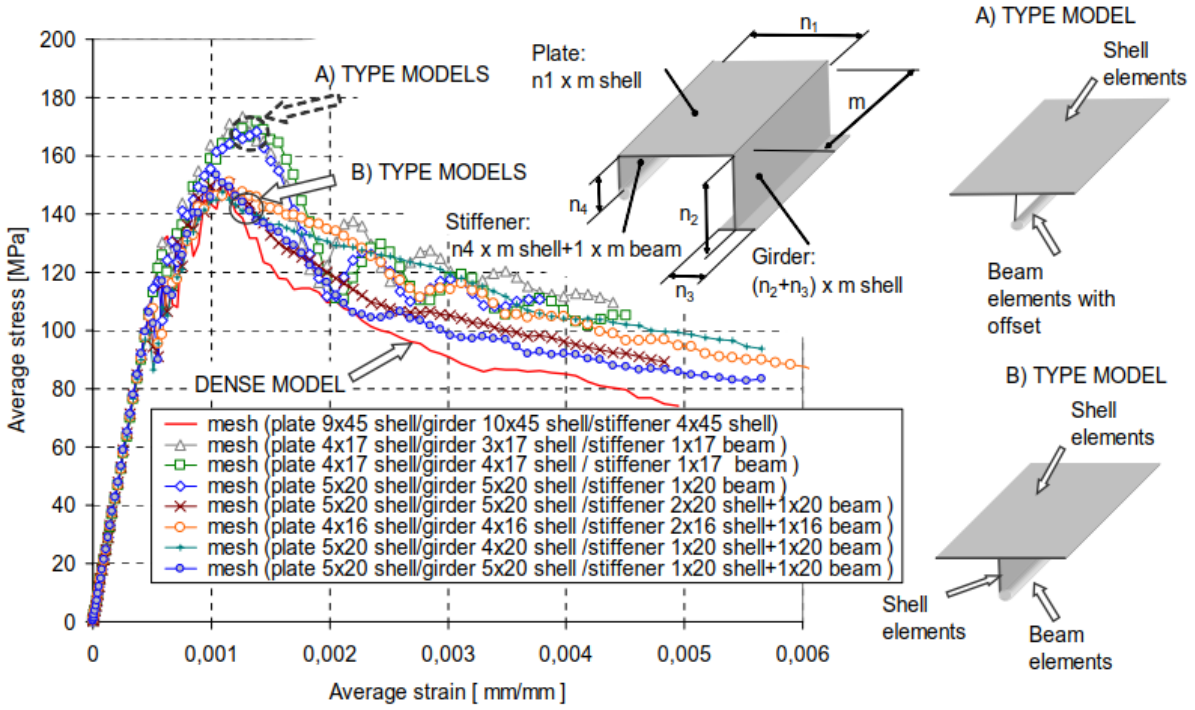

Figure 8. Comparison of various stiffened plate models in axial compression (Naar, 2006).

2.3.2. Loading and boundary conditions

In order to correctly reflect its behaviour, the vessels must be constrained by means of boundary conditions. Applying the correct boundary conditions is of vital importance, and if done correctly allows the user to take advantage of the symmetrical properties of a structure and greatly simply the model, which in turn reduces computing time. The objective of the boundary conditions for a global

model is to provide simple supports while avoiding in-built stresses and avoid rigid body motions. It is good practice to avoid setting fixation points at the centerline or at the extremities of the vessel (i.e. fore and aft) well distanced from “hot” areas of interest, where imbalances may induce singularities (DNVGL, 2016).

A combination of still-water and dynamic loads are usually applied when carrying out global analyses of passenger ships. The principle component of the still-water load is the light ship weight, which is usually achieved by creating as complete of a model as possible and assigning the correct density to the material, which in most cases consists of various types of structural steel. Various material densities can be used for each material type, in order to achieve the correct weight distribution. If some of the lightship cannot be modelled for one reason or the other, mass points can be connected to the structure with rigid body elements or springs. All additional heavy machinery and outfitting is also usually modelled (i.e. gensets, large cranes, etc.) as mass points and connected to the structure by the same means; another method is that of adding the masses in the form as surface loads on select areas. This allows to realistically determine centres of gravity and moments of inertia. The remainder of the still-water loads consist of buoyancy loads, which are applied to the wet part of the hull, deadweight or passenger loads (which can be modelled similarly to the machinery loads) and tank loads cause by the liquid masses (DNVGL, 2018).

Modelling dynamic loads requires either a rule based or a direct approach, the latter being more accurate and is based on equivalent design wave methods, utilizing values determined through direct wave load analysis. The former method consists of applying a pressure at the bottom of the FE model to the wet surface shell elements and trying to achieve a bending moment as close as possible to the required rule bending moment and shear force distribution (DNVGL, 2018*).

Due to the fact that the aim of the study is not to carry out a quantitative strength calculation but to understand the global structural behaviour, the secondary and tertiary effects from the loading and added masses will not be included, as they would tarnish the results with effects that are irrelevant for this case. A similar approach was taken by both Parmasto and Naar (Naar, 2006; Parmasto, 2012).

3. Case study

The ship structure concept used to carry out this study is that of a relatively modern Post-Panamax type passenger ship. Similar versions of this very structural concept have been used as reference model also in studies conducted by Naar, Lillemäe and Parmasto respectively, as it provides a good example of a modern passenger vessel containing all the modern structural characteristics and layout of this ship type (Naar, 2006; Lillemäe et al, 2014; Parmasto, 2012). Modern classification society deck strengthening recommendations, aligned with the ULS and SLS principles, are followed in this version of the same structural concept (DNVGL, 2018). The three-dimensional finite element model was created using the commercial software FEMAP 10.1.1.

This considered passenger ship is made up of a double bottom, thirteen decks and where the superstructure and main deck meet, a recess for lifeboats. The upmost deck has a boxlike structure, with the intent of providing additional bending stiffness to the hull girder, when she is subject to global bending. The decks on the lower part of the ship are supported by pillar lines and the side shell, while in the superstructure, starting from the 9^{th} deck up to the very top, longitudinal bulkheads are present. These are placed at a distance of 4000 mm from the centreline. Also starting from the 9^{th} deck upwards, the side shells have large openings measuring 2200 by 2100 mm. Web frame spacing is set as 2730 mm. Twenty transverse watertight bulkheads divide the bottom part of the ship up to the 7^{th} deck, while the reminder of the decks have six fire bulkheads.

In this structure type, the shear load is carried by the side shell in the lower parts of the ship up to the 7^{th} deck, by the side shell of the recess space from the 7^{th} to the 9^{th} and primarily by the longitudinal bulkheads in the superstructure, sure to the presence of large openings in the sides. The thickness of most decks is of 5 mm, with a few exceptions. The bottom three decks have a thickness that increases incrementally downwards from 5.5 mm to 7.5 mm. Deck 9 has a thickness of 7 mm from the side shell to the longitudinal bulkhead and of 5 mm from bulkhead to centreline. The longitudinal bulkhead is 6 mm thick and is stiffened by HP100 profile, which are also used to stiffen the decks. Most decks have longitudinal girders made up of a flange of 200x10 mm and a web of 480x 8 mm. Side shell thickness varies too, with the plating in the lower bottom of the ship having a thickness of 16 mm, of 15 mm and 14 mm between the 5^{th} and 6^{th} decks and of 13 mm in the recess area. Figure 9, shows the generic layout of the midship section of the vessel, with a more detailed version with visible scantlings available in appendix 1.

In order to take advantage of the symmetric properties of the ship's structure and significantly decreasing the required computing time by reducing the number of elements present, a simplified model is used. The smaller number of elements present, in turn, allows to refine the mesh in specific areas of interest to obtain better results, such as the panels present at midship; these areas are illustrated in Figure 10. The simplified structure consists of a quarter model, in which both fore and aft were removed, with section planes placed at midship and along the centreline.

The offset beam technique, which was briefly described earlier, was used to model the secondary stiffeners. This method was chosen over the equivalent shell element one, as it allows for a better comparison with the results obtained using a similar approach in relevant reference studies, some of which are mentioned in the initial paragraph of the section. The stiffener's web is modelled using four-noded rectangular S4 shell elements, while two-noded B31 beam elements make up the flange. Parmasto noted that since the resulting aspect ratio secondary stiffeners' web is considerably poor

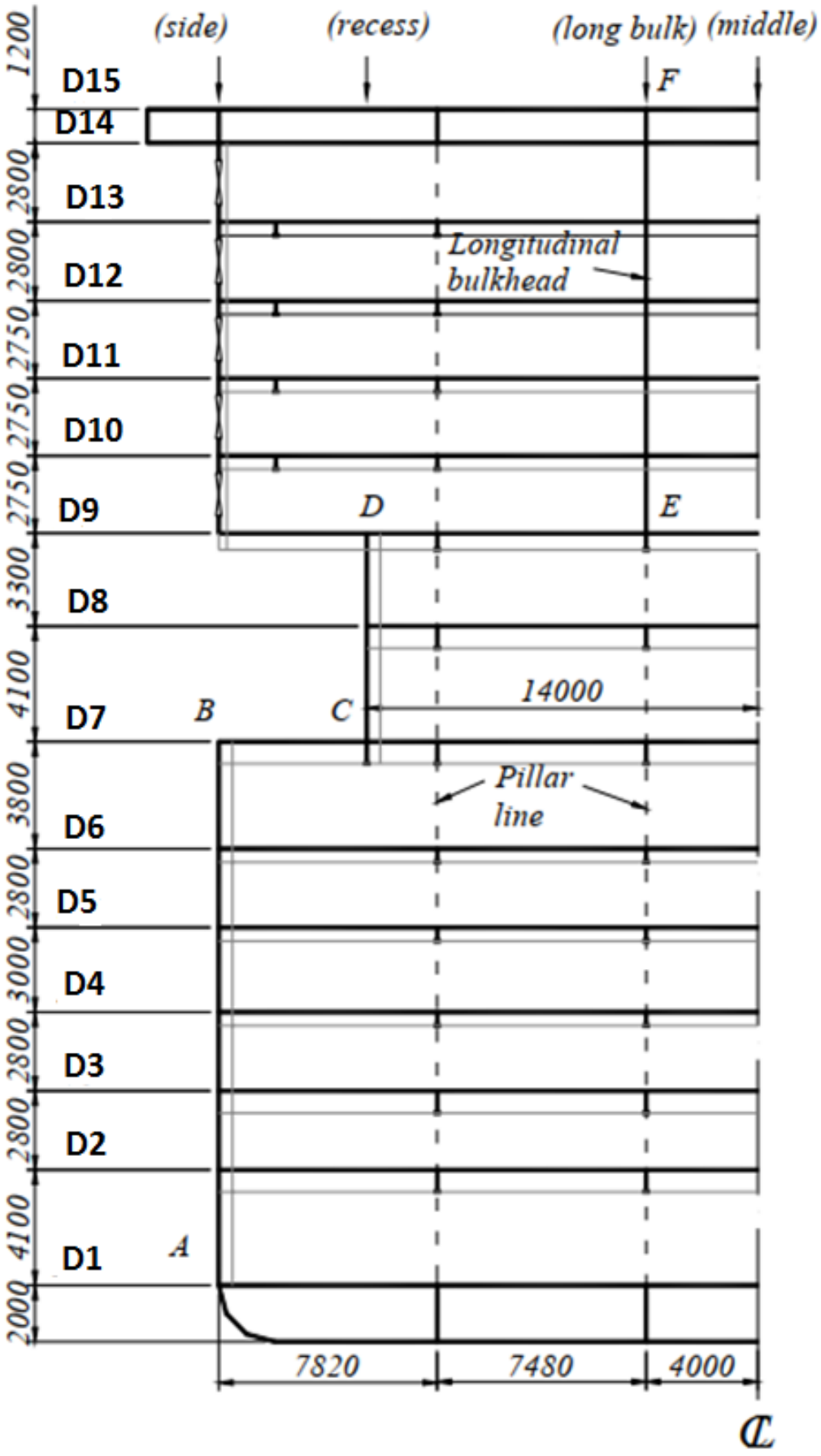

Figure 9.Generic layout of the midship section for the Post-Panamax passenger ship.

(0.0176 – 0.0733), the stiffeners are vulnerable when subjected to in-plane bending, which would be potentially exacerbated by the loss of stiffness of the panels. However, the fact that only a global scale investigation is being carried out and the structure will primarily be subjected to vertical bending due to the nature of the applied load, reduces the negative consequences of the relatively poor aspect ratio, since the tertiary effects are not the subject of the study (Parmasto, 2012). In the study, 5x20 and 3x20 shell elements are used in plate strips and girders respectively. For plate stiffener webs, 1x20 shell elements are applied. Primary stiffeners were modelled using four-noded quadrangular S4 elements for both web and flange, which resulted in a better aspect ratio (0.33 circa) for longitudinal girders. Pillars were modelled using two-noded B31 beam elements.

Figure 10 illustrates the mesh used in the study. This study hopes to recreate the realistic response due to shear loading of structures which will primarily carry this type of load, such as side shells (especially in the discontinuous recess area connecting the hull and superstructure), decks and longitudinal bulkheads. Naar demonstrated that the shear forces flow chiefly along the path marked by the letters ABCDEF, as shown in Figure 9, and are of highest magnitude at the following ship

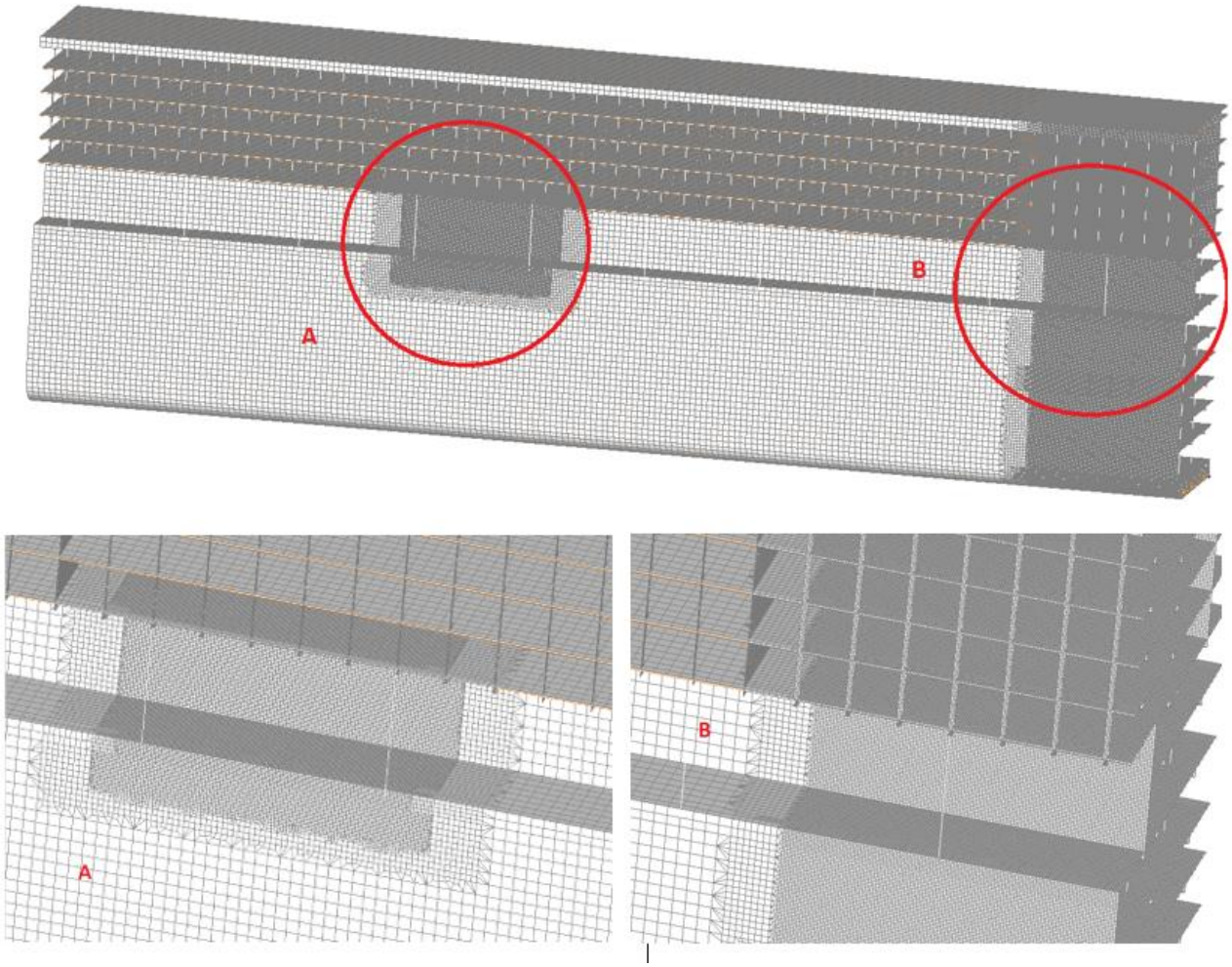

Figure 10. Mesh of entire model (Top) and finely meshed zones with transition areas: L/2 (B: Bottom right) and 3L/4 (A: Bottom left).

lengths: x=L/4, x=L/2 and x=3L/4 (Naar, 2006). In order for these structural elements to accurately portray the occurrence and effects of shear buckling, a relatively finer mesh is necessary along the whole ship length for those structures would be necessary. However, this would dramatically increase the problem size and consequentially the required computing capacity. Therefore, only the areas where the shear stresses are expected to have maximum values will be refined; these are

indicated by the letters A (x=3L/4) and B (x=L/2) in Figure 10. A comparatively finer mesh was also used for the stiffened decks amid ship, for the same reason. The resulting mesh contained 190887 two-noded beam elements and 779107 S4 elements, of which 771180 were four-noded and 7927 three-noded. Rigid body elements were also used in the transition zone between fine and coarse mesh zones, to ensure the stiffener webs would maintain realistic behaviour where connected to beam elements of the coarse areas, at their extremity. This resulted in a combined total count of 970577 elements.

A sinusoidally distributed pressure load was applied onto the wetted surface of the model, in order to recreate the bending moment and shear forces. This is a slightly simpler approach than that suggested by the classification societies, where a number of still-water loads are required (i.e. machinery, outfitting, tanks, deadweight), in addition to dynamic loads (DNVGL, 2018). These loads were omitted as the study's aim is only to recreate the sagging condition and the qualitative added value would be limited. Symmetric boundary conditions were applied at midship and along the centreline, in order to prevent axial anti-symmetric collapse modes of some components. The first set of boundary conditions is applied along the centreline where the ship structure has been sectioned, constraining its rotation around the axis perpendicular to the said plane, and its translation in both directions along this plane. The second was applied to the plane at midship, restricting translations in the vertical direction. The final constraint set only permits translation in the vertical direction and was applied to the edge nodes of the hull's outer shell. As material, linear elastic steel linear was assigned, with a Young's modulus of E = 206.8 GPa and a Poisson's ration of ν = 0.3.

3.1. Post processing

The FE code will provide numerical values as output through which the post-processing tool, in this case FEMAP 2020.1, will extract nodal displacements and the various stresses in each individual element. The following paragraphs will outline how this information will be used for better understanding the structural behaviour of the vessel when the elastic buckling phenomenon is included.

3.1.1. Displacements

The goal of this analysis is to qualitatively verify the extent to which changes in stiffness, due to the inclusion of the elastic buckling behaviour at sub-critical load levels, affect the entire structure's response. A good display of changes in stiffness can be obtained by the comparison of deflection levels of certain nodes, placed at telling locations of the structure. Obtaining quantitatively correct deflection levels would be more of a challenge, as the bending stiffness formulations of classic beam theories (i.e. Euler-Bernoulli and Timoshenko) are inapplicable to the studied structure. This is due to the departure from those theories' required assumptions, mostly due to the warping of the cross section of the vessel, as Bleich noted already in the second half of the last century (Bleich, 1952). Another shortcoming is the assumption that all fibers (i.e. decks) in Timoshenko's theory deflect by the same amount (Romanoff et al, 2013).

Nevertheless, qualitatively speaking, investigating deflections can provide insightful knowledge on the kinematics occurring during the deformation process. For example, observing the change in vertical deflection of certain decks as the cross-section of the investigated structure, provides a valuable insight on the mechanisms of the hull-deckhouse interactions. Under sagging conditions, the superstructure tends to rise out of the main deck at mid ship and sink into the hull further along the ship length. By measuring the displacement of the side connection point of the superstructure and the hull, useful information regarding this interaction can be obtained, as was observed by Parmasto. The presence of a longitudinal bulkhead and a pillar line extending throughout the hull provides the necessary structural continuity; point D in the left side of Figure 11 illustrates the mentioned location for the m2cell structure in Parmasto's work, but point A is suitable for the model used in this study (Parmasto, 2012).

Furthermore, in order to identify the instance in which elastic buckling occurs in order to narrow the scope, plotting the deflections against the moment values of the hull girder sagging proves to be useful. Areas worth investigating under these conditions are the upper decks are in compression, the bottom half in tension or the discontinuous side, in order to see the amount by which the stiffness reduces, before plasticity is reached. The areas can be in right side of Figure 11. The deflection of the individual panels in those areas, can also be investigated for a more localized understanding of the behaviour. This approach was also found useful in several publications investigating the ultimate strength limits of passenger ships (Naar, 2006; Andric & Zanic, 2010).

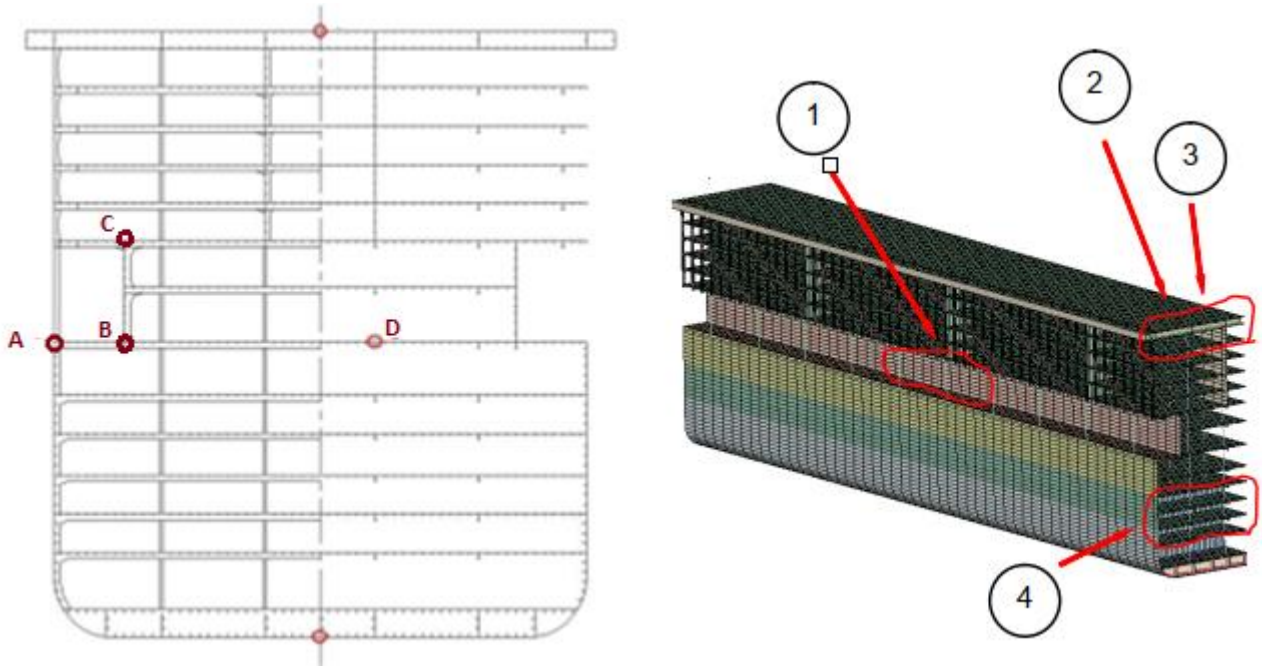

Figure 11. LEFT: Investigated points (Parmasto, 2012); RIGHT: Areas of interest (Naar, 2006).

3.1.2. Stresses

Classically, the distribution of normal strains over the ship structure's height had been the primary method of analysing the ship response when subjected to longitudinal bending due to sagging. After having been proved to be inadequate for multi-deck housed passenger vessels, attempts to re-adapt beam theories to derive the strains were made (Bleich, 1952). Sectioning a passenger vessel

subjected to longitudinal bending along its length, an observer would notice that the distribution of normal strains in each deck of the superstructure varies along both height and width. Therefore, even theory of elasticity-based methods developed subsequently proved to be inadequate, as they contained the assumption of uniform normal strain distribution along decks (Parmasto, 2012). A numerical three-dimensional FE method such as the one used in this study does not incur in this particular shortcoming and conveniently uses the average normal strains of each plate to derive their average normal stresses. These are more useful from and engineering perspective, as they give a clearer indication as to the usability of plates, not to mention using limit state setting guidelines suggested by classification societies (DNVGL, 2016).

As already mentioned, the goal of the study is to investigate eventual changes in the global behaviour of the structure due to difference in two sets of in material behaviour, which would make the primary type of stress of interest the membrane stresses present in the various decks. Averaged membrane stresses are retrieved from the middle integration point over the elements' thickness. This means that at each deck, the average of normal stresses is derived by using the normal stresses of each plate's top and bottom (Palm, 2015). Shear stresses at critical locations would also be informative, with particular attention being reserved for critical locations such as the hull's side shell and longitudinal bulkheads. The changes in shear stresses at the locations are a good indicator of changes in the load carrying mechanism of the structure as a whole, providing useful insights on the possible effects of buckling due to loss in stiffness.

However, as the investigated load levels are limited to ranges capturing only elastic buckling, a comparison of stresses using the two different approaches won't be displayed in this study. This is due to the lack of significant changes in the load carried by the individual elements, nor will there be a comparison of different structures (shape or dimensions) as was the case in the studies carried out by Parmasto or Lillemäe, in which case these differences would arise (Parmasto, 2012; Lillemäe, 2014). The stresses calculated using nonlinear and linear methods would therefore not change significantly, making the task futile, as the necessary understanding of the behavioural changes can best be achieved by analysing changes in load distribution. A more useful task would be to compare the stresses at which the structure buckles to the buckling limits provided by classification society guidelines; this will be presented.

3.1.3. Forces and Moments

The decks of the superstructure of the investigated structure and its composing elements will be the primary recipients of the compressive loads caused by the bending moment they must withstand, being relatively thin by necessity. Once the normal stresses of the decks have been determined, the membrane forces acting on said elements can be calculated. This, in combination with information regarding the response of the beam elements representing the stiffeners and amount of load carried by longitudinal shell elements, enables the moment carried by the hull and superstructure respectively to be calculated.

As seen in various relevant studies, understanding the force distribution of the individual structural elements and witnessing their eventual change, will shed light on the eventual occurrence of load-shedding and if the changes in stiffness due to elastic buckling affect this (Lillemäe et al., 2013; Lillemäe et al., 2014). A qualitative analysis of the redistribution of loads would be beneficial for

evaluating possible over/underestimations during the dimensioning of stiffening elements at various hierarchical levels, which could significantly impact future design choices, as seen in Palm's work (Palm, 2015).

4. Results

4.1. Response comparison

4.1.1. Deflections

The loading path and failure modes caused by the sagging condition are illustrated in Figure 12. Initially, achieving a moment value of 5,00E+06 kNm was the target. Naar's work, using the same hull girder concept structure, had shown that within this load range, both elastic shear buckling of side plates at the recess area at x = 3L/4 and elastic plate buckling of the upmost deck at midship could be captured. Higher moment values edging nearer to the ultimate moment value, which for this structural concept had been shown to occur at around 8,30E+06 kNm, were never intended to be reached. This is because the purpose of this study is to study the effects elastic buckling of the hull girder on a qualitative level, which could be achieved within the aforementioned range (Naar, 2006).

Time and computational power capacity limitations hindered the ability to go beyond achieving a moment of 2,88E+06 kNm. The results show that elastic buckling occurs at far earlier stages of loading that expected, when compared to the findings of Naar. The first decks to show signs of failure are deck 5, around the area where it is supported by the transverse bulkhead, and deck 9 of the superstructure. Deck 9 buckles specifically at the innermost section of the deck flanked by the longitudinal bulkhead and centreline. The relatively unsupported and slender deck 7 buckles next, with the topmost deck (deck 15) being the final one for which an elastic buckling response can be observed within the set range. There appear to be no effects on the global stiffness of the hull girder due to the elastic buckling of these decks. The model's decks buckled when subjected to stresses which closely correspond to the limit stresses calculated using class society guidelines (DNVGL, 2015*).

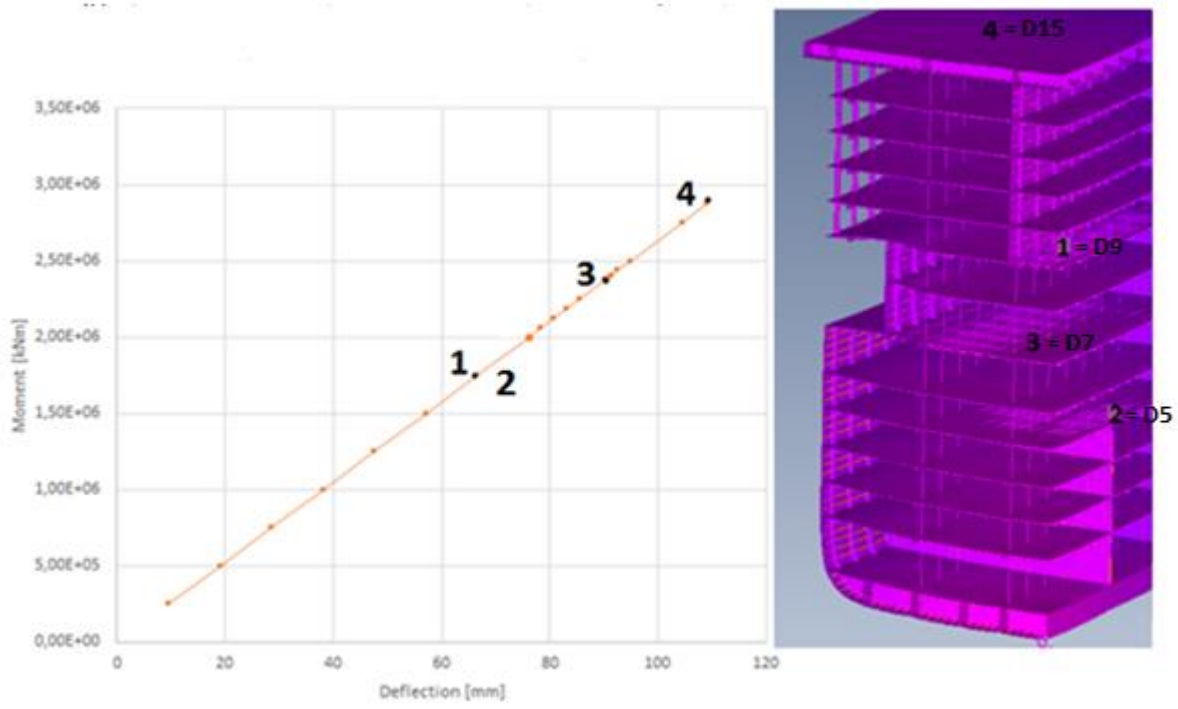

In order to clearly understand the individual buckling modes of the deck, it is helpful to keep in mind the global dynamics of the hull girder, the superstructure and how they interact. These topics had already been touched upon in previous parts of this study. Bleich had already shown how this behaviour can be described by idealizing the hull and superstructure as two connected and individual beams. Figure 13 illustrates the resulting effects the combination of these phenomena has on the structure at midship.

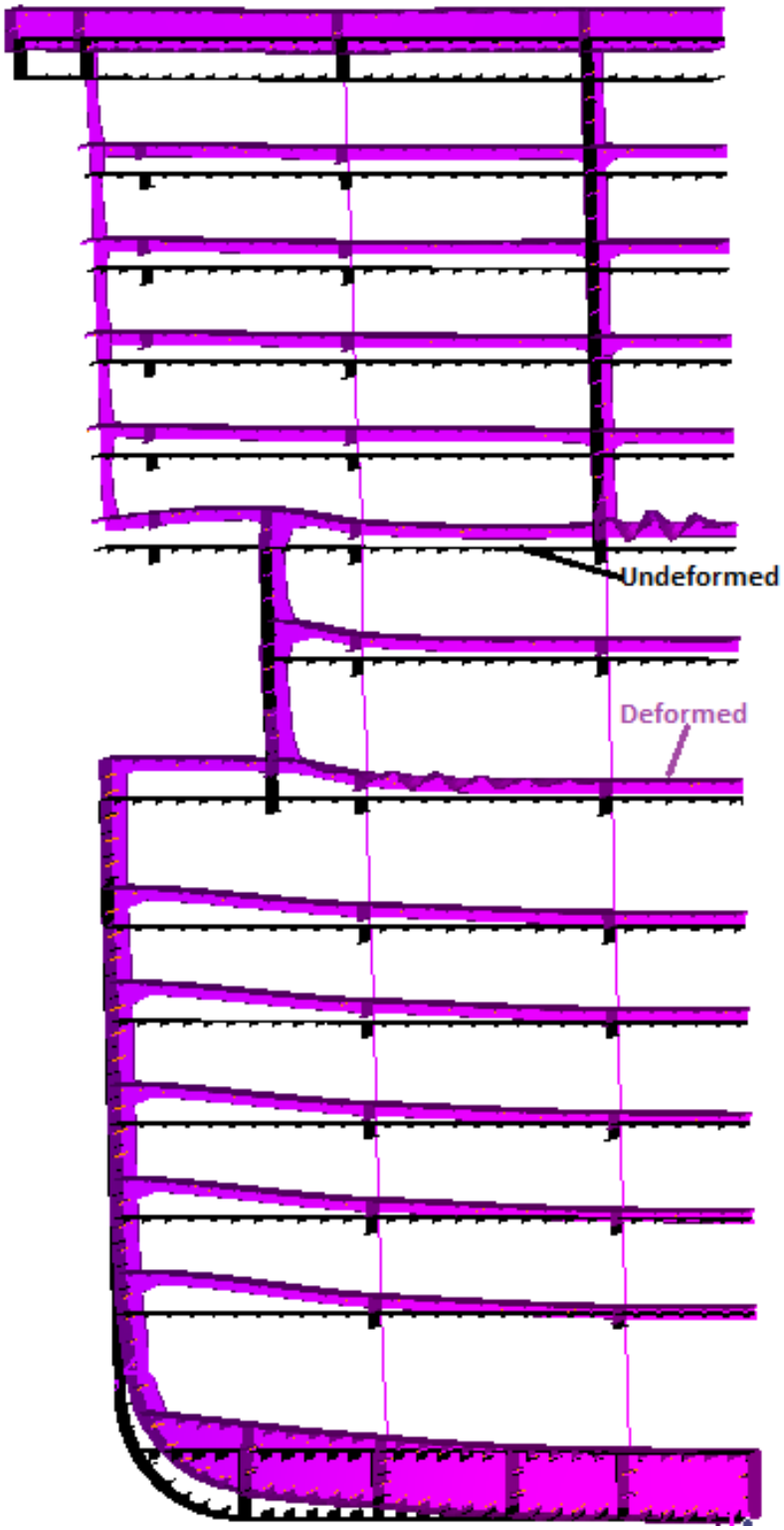

Figure 13. Deformed vs. undeformed structure of the web frame at midship.

As already stated, the first part of the structure to buckle elastically is the section of deck 9 flanked by the longitudinal bulkhead of the superstructure and the centreline. This deck is subjected to both transverse and longitudinal compression. The transverse one is caused by the combination of the vertical pressure load being transferred through the pillar line into the bulkhead and the opposing vertical force acting at the connection between hull and superstructure. Longitudinal compression is caused by the sagging condition, due to which the superstructure decks are being compressed longitudinally. The effects of the latter compression though, are playing a secondary role at best at this degree of load magnitude, as shown by the fact that buckling in fact occurs due to the transverse compression. See Figure 14.

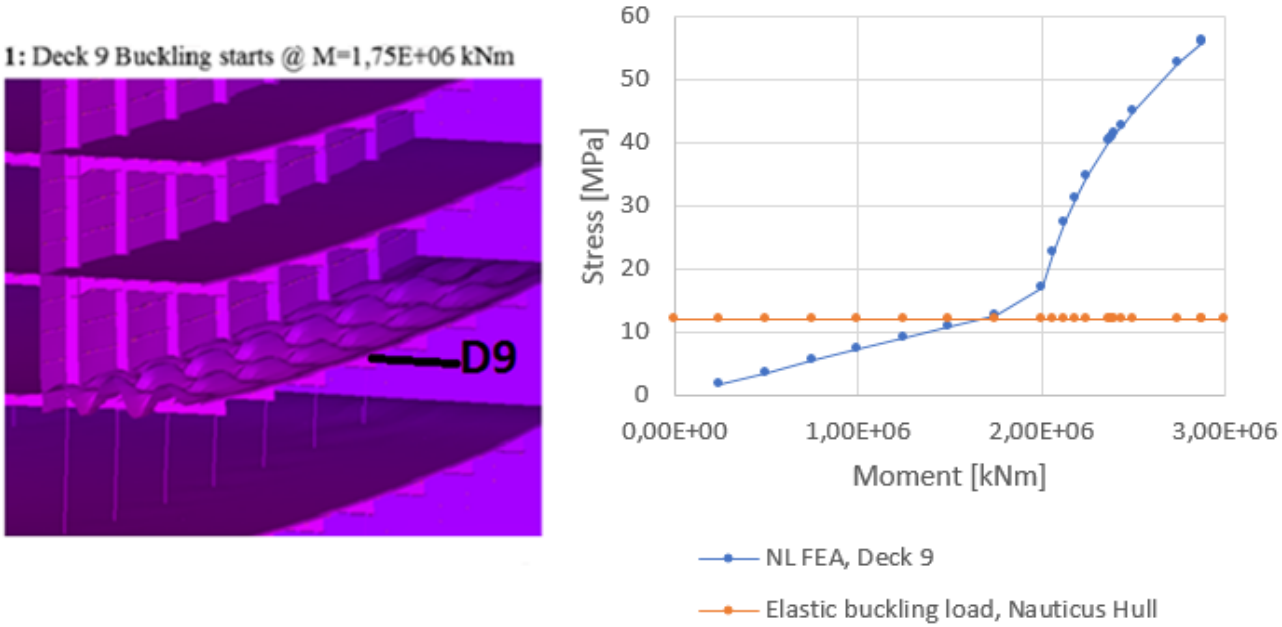

Figure 14. Individual buckling mode of Deck 9 and comparison to transverse buckling stress limit from Nauticus Hull.

As can be observed in Figure 15, Deck 5 shows signs of elastic buckling at the same load step as the previously described deck. Buckling initiates at frames 4 and 5 contemporarily, with longitudinally adjacent plates gradually following at subsequent loading steps. The partial transverse bulkhead can

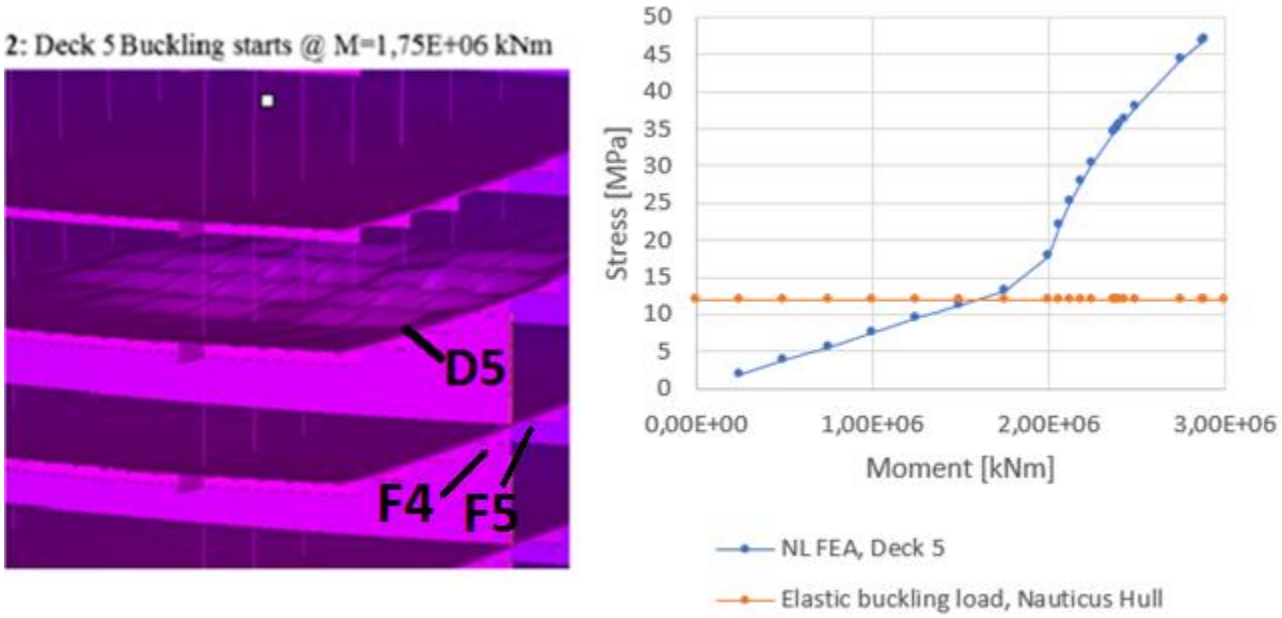

be thought of as the web of and I-beam, of which deck 5 and the upmost deck of the double bottom (deck 1) are the I-beam's flanges. The upmost flange (deck 5), can be conceptualized as pinned at its extremities by the full bulkhead on one side, and the midship symmetry constraint on the other, creating a scenario in which the lower flange (double bottom) is being pulled downwards by the pressure load while the pins resist the movement. This load will act through the web of the I-beam (the partial bulkhead) and the deck will bend transversely along a longitudinal axis, perpendicular to the partial bulkhead, causing it to buckle. If the applied load were to increase, more frames would buckle in the same fashion, eventually reaching the transverse bulkhead and midship.

The buckling of deck 7 (the boat deck) is another example of the previously described global load carrying mechanism in action. The connection point between hull and recess area is visibly rising, as can be seen by the markedly visible deformations in the section of the deck between the longitudinal girder furthest from the centreline and the outer shell of the recess area. Meanwhile, the pillar lines flanking the area of the deck delimitated by longitudinal girders, pull the deck downwards, driven by the pressure load acting at the outer shell of the double bottom. The deck is subjected to compressive loads acting transversely, while also being in compression longitudinally at higher loads, the latter being due to the nature of the sagging condition. Frames 6 and 7 of the deck, flanked by the pillar lines, are where the buckling initiates, gradually spreading towards midship, as shown in Figure 16. At subsequent load steps, a shear buckling mode can also be observed in the area of the deck between the outer shell and the pillar line closest to it. This is a consequence of the combined effects of the deck being in compression and the connection between recess area and hull being subjected to shear. The deck plates initially exhibit buckling in the transverse direction.

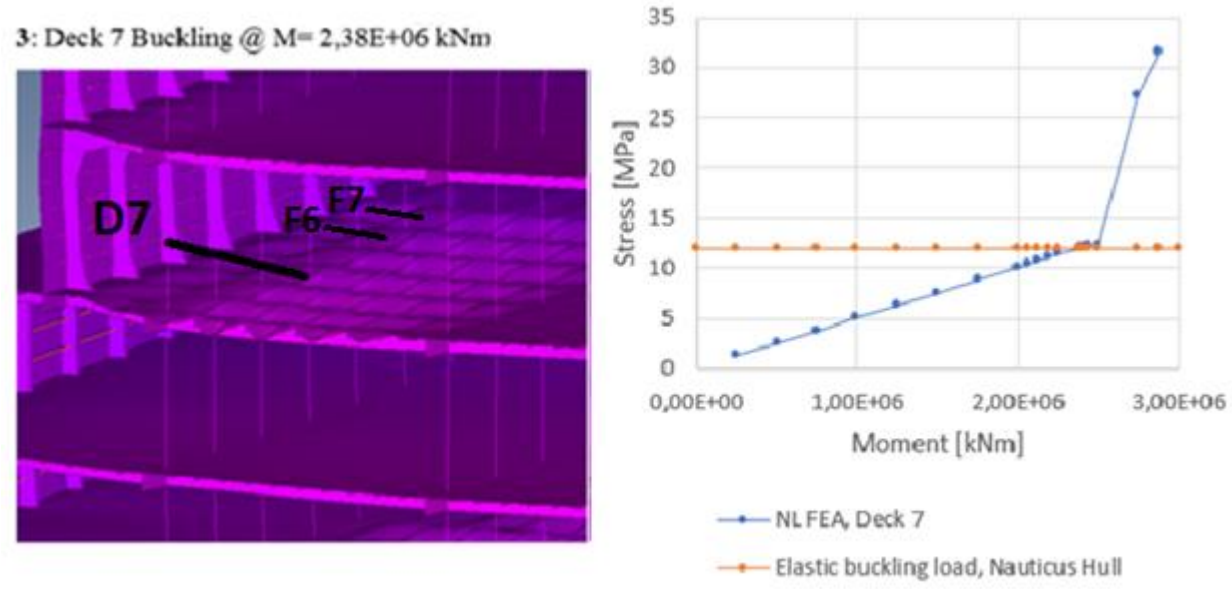

Figure 16. Individual buckling mode of Deck 7 and comparison to transverse buckling stress limit from Nauticus Hull.

The sagging condition causes the topmost deck (deck 15) to be subjected to the greatest longitudinally compressive loads of all, relative to the other decks. This deck is the only one to buckle in the longitudinal direction. The onset of elastic buckling by bending, caused by this longitudinal compression, occurs at the last load step which could be achieved; its effects are visualized in Figure 17.

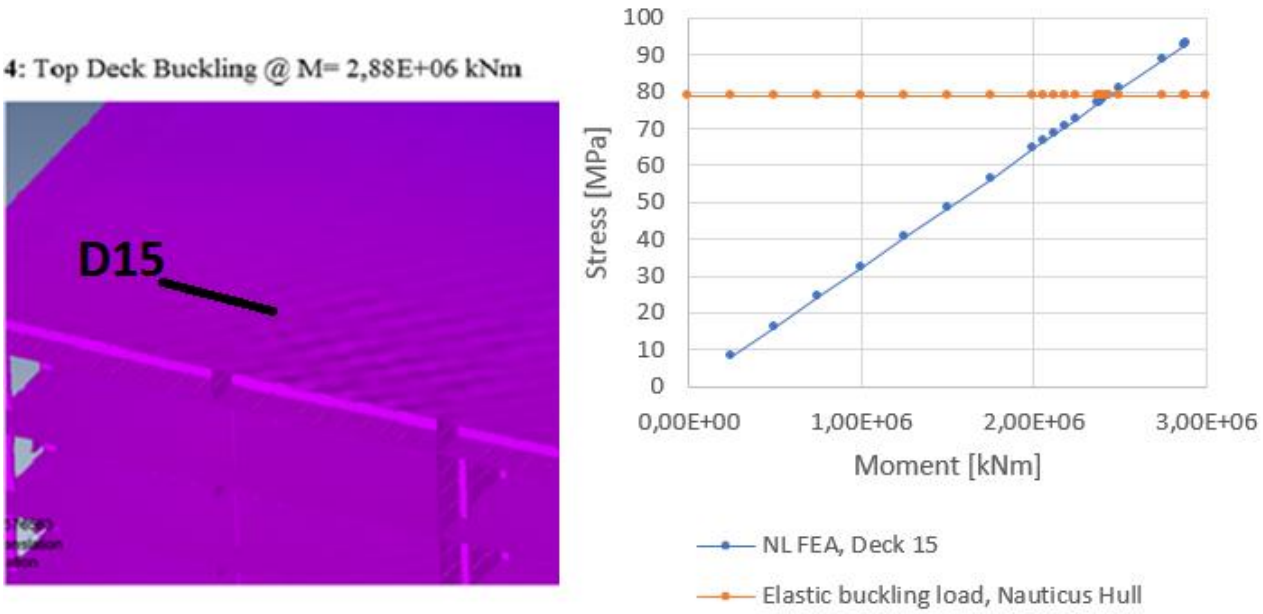

Figure 17. Individual buckling mode of Deck 7 and comparison to longitudinal buckling stress limit from Nauticus Hull.

4.1.2. Vertical deflections of points on decks along the x-axis

In order to further investigate whether significant qualitative changes occurred in the global behaviour of the hull, the vertical deflections of certain points using the nonlinear and linear solving methods were compared. The exact locations of points A, B and C are represented below.

Both Figure 18 and Figure 19 indicate that using either linear and nonlinear approaches results in no significant difference. A maximum difference of 0,23 mm in vertical deflection values at x=L, which is less than 0,1% of its respective deflection value, is reached. In each of the two cases, the superstructure can be observed to be rising out of the hull at midship, while the opposite is shown to be the case as the end of the structure is approached.

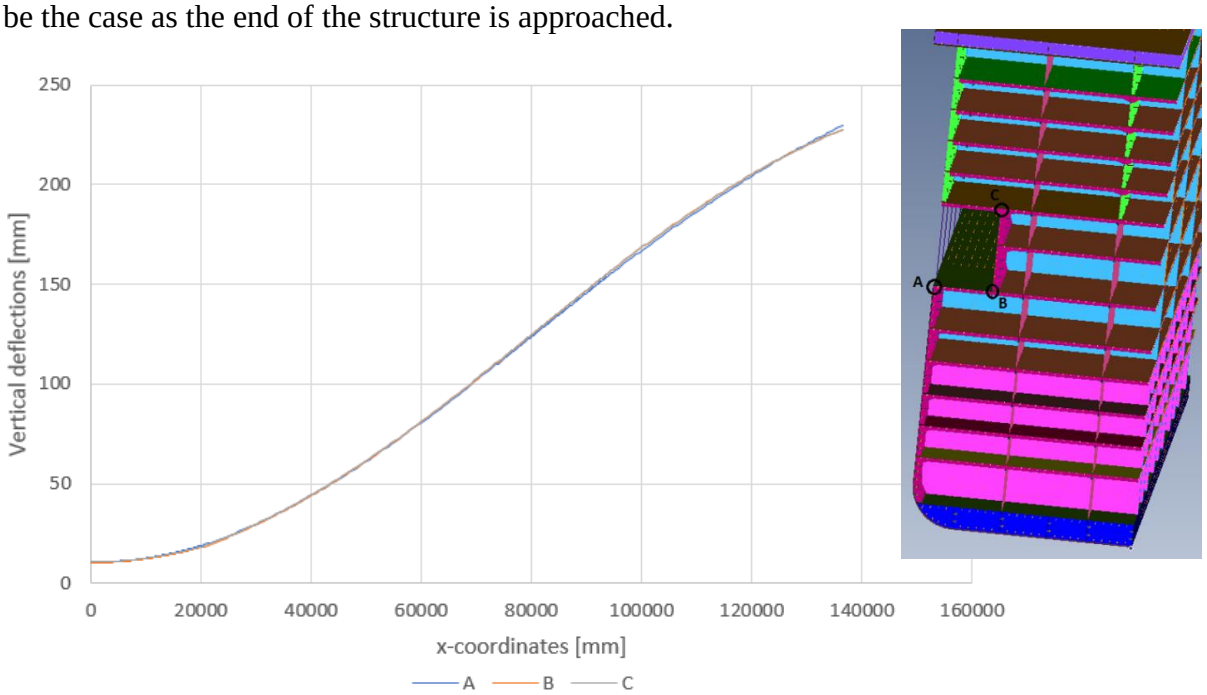

Figure 18. Vertical deflections of decks along ship length using a nonlinear approach at points A, B and C.

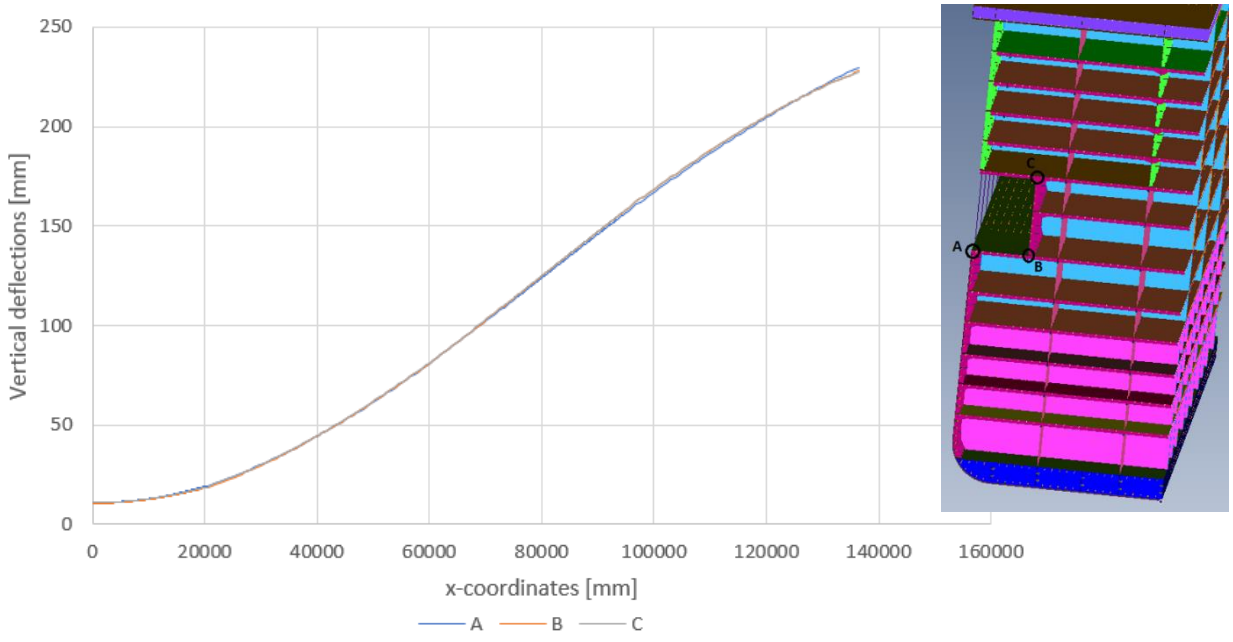

Figure 19. Vertical deflections of decks along ship length using a linear approach at A, B and C.

4.1.3. Forces at each deck and its components

A comparison of deck force distributions at x=L/2 and x=3L/4, calculated using the nonlinear and linear approaches respectively, is given in Figure 20. This is the first step used in understanding the load carrying mechanism and carry out a comparison. As can be expected when a vessel is sagging, the results show that the lower decks are in tension while the opposite is the case for decks in the upper direction, which are in compression. The idea that the decks carrying the most load are the ones at the vertical extremities of the structure is also confirmed.

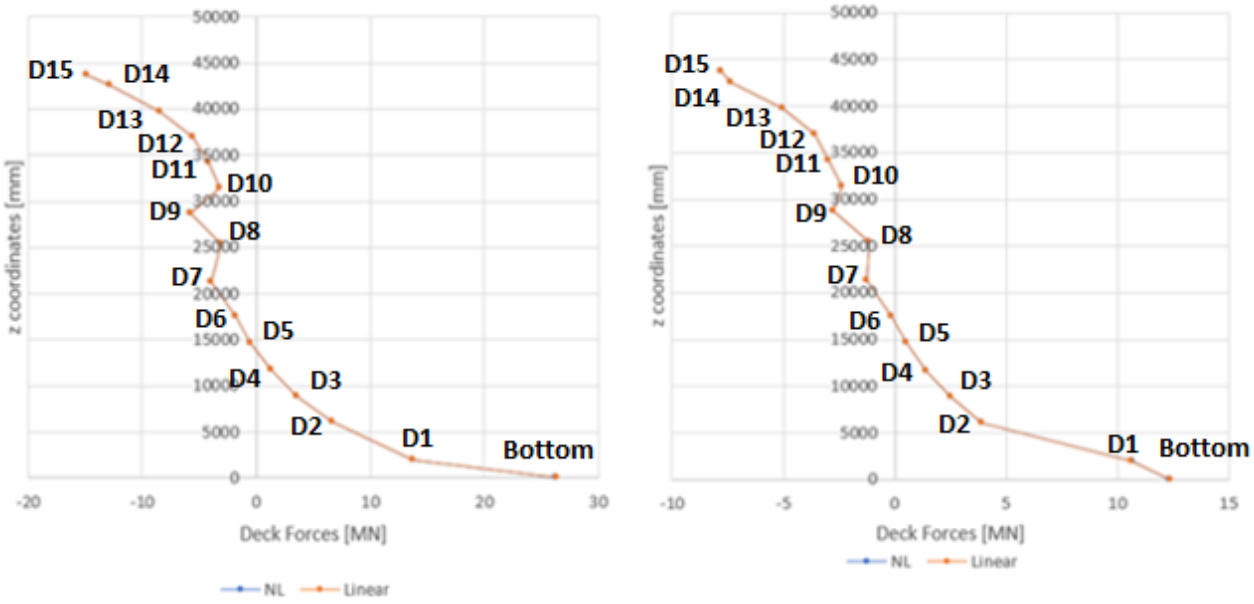

Figure 20. Comparison of deck forces using NL vs Linear approaches at x=L/2 (LEFT) and x=3L/4 (RIGHT).

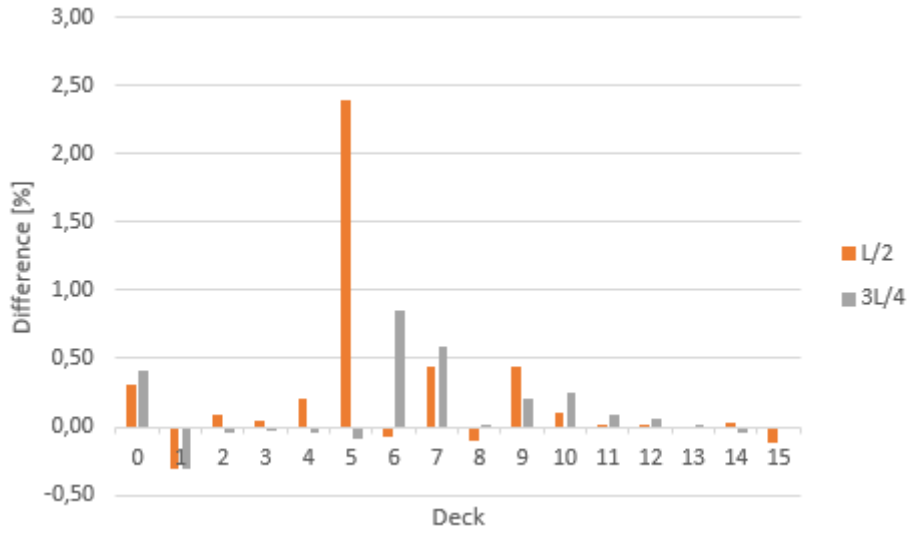

Figure 21. Difference in forces [%] between NL and Linear approaches at each deck.

There appears to be no true major deviation between the nonlinear and linear models, with the exception of a 2,5% difference in deck 5 at mid-ship, as shown in Figure 21. This doesn't come as a surprise, deck 5 being amongst the decks having been found to extensively buckle elastically within

this load range. In order to fully grasp the load carrying mechanism of the deck and how it changes as the deck gradually buckles and loses stiffness, the force distributions of the individual structural components are presented in the following paragraphs.

The axial forces acting on this deck's individual components (deck 5) are presented in Figure 22. Differences in force magnitude can be noticed when comparing the two approaches, with less load being carried by the deck's plate, stiffeners and girder furthest from the centreline when the nonlinear method is used. The longitudinal girder closest to the centreline, which is also the one nearest to area of the deck where the buckling initiates and is more "severe", carries a greater share of the load after buckling, once geometric nonlinearities are considered.

The linear model appears unable to capture these effects, grossly misestimating the loads acting on the longitudinal deck girders, as shown in Figure 23. The differences in calculated load reach up to 85%. It's worth nothing though, that this is also due to the force magnitude being relatively small in the first place, meaning that a small change in magnitude corresponds to a very large change in the percentage. The deviations are also significant for the deck plate itself and the stiffeners, with differences in values of 2,4% and 7,3% respectively. The changes in load carrying mechanism captured, strengthen the case for the validity of the method employed.

	Plate	Stiffeners	Girder 11480mm from CL	Girder 17600mm from CL
NL [kN]	-518,90	-33,91	4,07	-0,13
L [kN]	-531,62	-36,75	2,74	-0,92

Figure 22. Total axial force carried by deck 5 components.

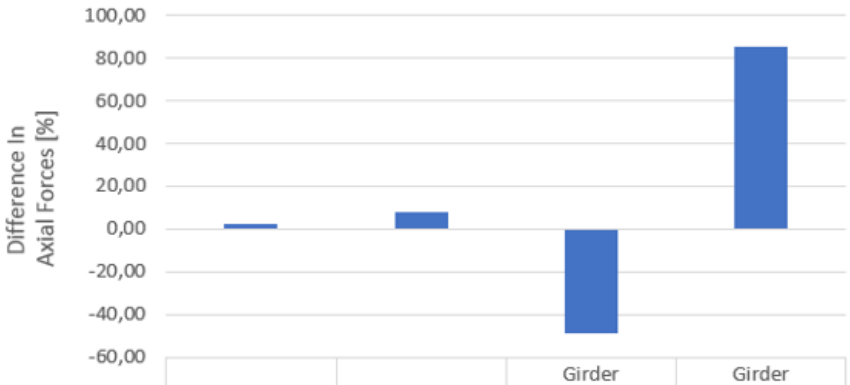

	Plate	Stiffeners	Girder 11480mm from CL	Girder 17600mm from CL
Difference [%]	2,39	7,73	-48,73	85,54

Figure 23. Difference [%] between NL and linear approaches.

Taking a step further into detail, if the step by step increase in axial load of each component is plotted for both linear and nonlinear methods, it is possible to clearly distinguish the bi-linear behaviour characteristic of elastic buckling, especially for the girder closest to the centreline. The behaviour matches linear elastic behaviour until the buckling is initiated, which for deck 5 occurs at a value of 1,75E+06 kNm. The deck plate and stiffeners (Figure 24) then shed their loads primarily to the girder seen in the left of Figure 25. The behaviour of the girder 17600mm from the centreline is less clear and exemplary of this load shedding behaviour described this far; as it appears to not only decrease the rate at which the load is applied, but to also lose its load carrying capacity altogether. This might be due to its distance from the origin of where the buckling is initiated, implying that the other supporting structures closer to this location (girder 11480mm CL and partial bulkhead) carry a proportionally far greater share of the load once the deck plate and its stiffeners lose stiffness.

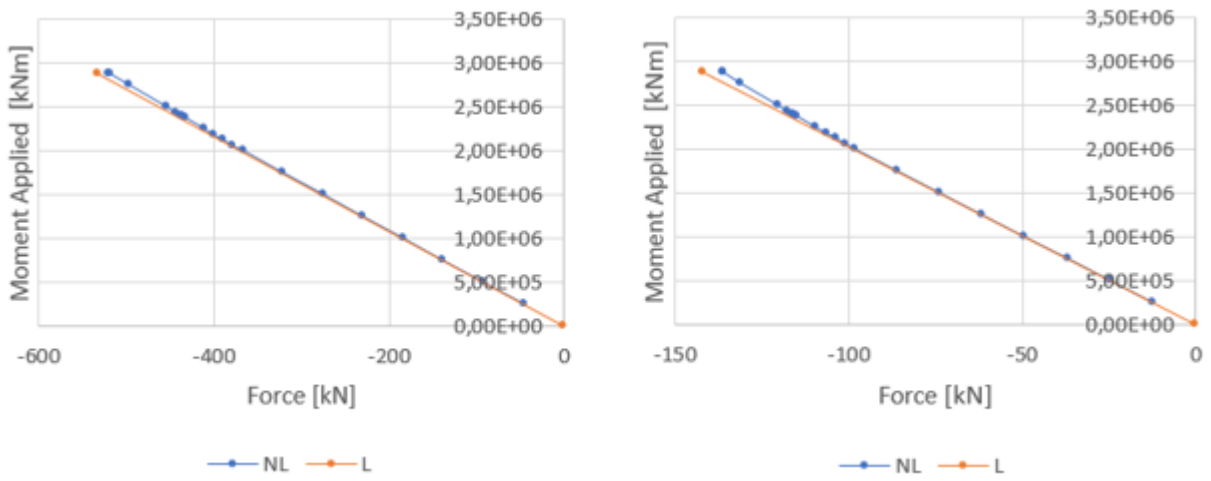

Figure 24. Step by step increase in axial force [kNm] of individual deck components: Deck Plate (LEFT) and Stiffeners (RIGHT).

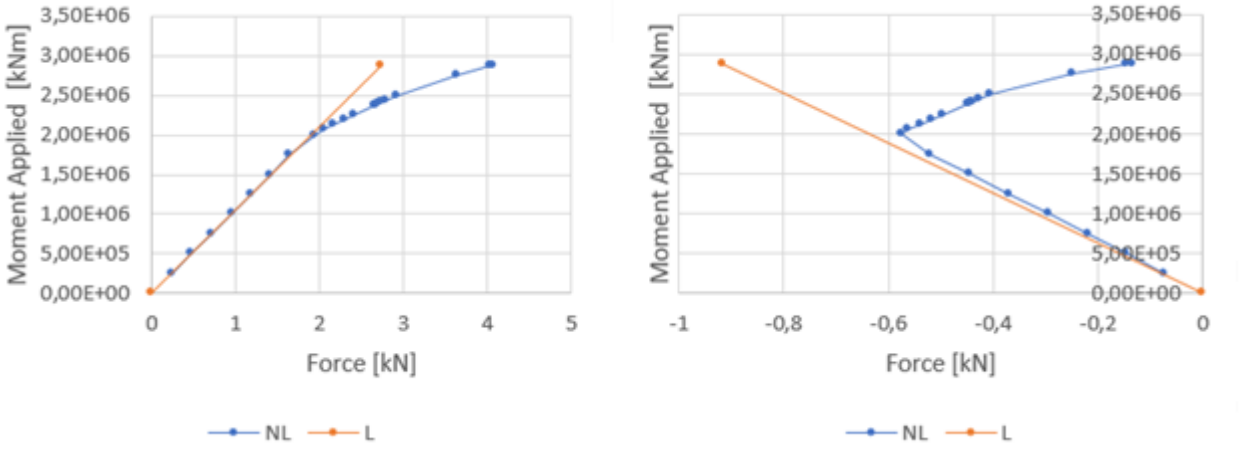

Figure 25. Step by step increase in axial force [kNm] of individual deck components: Girder 11480mm from CL (LEFT) and Girder 17600mm from CL (RIGHT).

5. Discussion

The employed modelling techniques proved capable of achieving the primary set objective of effectively and realistically capturing both the load carrying mechanisms of a modern passenger ship and recreate the load shedding mechanism of secondary and tertiary structures occurring due to the onset of elastic buckling at sub critical loads. The buckling modes of the stiffened deck panels were also correctly exhibited, matching the findings obtained through the extensive testing of the 70s and 80s (Smith, 1975; Smith, 1977). This claim is supported and strengthened by the similarity in the overall structural behaviour at various hierarchy levels to both theoretical models and similar related recent studies, such as the ones by Ekman, Lillemäe et al., Palm, Parmasto, Romanoff et al. and others that have been mentioned/referenced in this report (Lillemäe et al, 2014; Palm, 2016; Parmasto, 2012; Romanoff et al., 2013; Ekman, 2020).

Notable differences with Naar's study case with a very similar ship structure subjected to sagging condition were found. The most important of which being the load levels at which elastic buckling of decks were found to occur, with the first instance of elastic buckling behaviour being observed in the topmost deck, as opposed to decks 5 and 9. Shear buckling of the side shell of the recess area had also been observed by Naar, which wasn't the case in this study. There are no traces of elastic buckling behaviour of deck 5 either in that study, at least before its ultimate collapse. Decks 7 and 9 too display no signs of elastic buckling in the dissertation, as can be seen in the moment-deflection curve in Figure 3 (Naar, 2006). Overall, the behaviour of the hull girder structure used in this study appears to be stiffer than that used by Naar. This is understandable, as some of the deck plates were modelled as thicker; namely decks 9, 14 and 15, which have thicknesses of 7 mm, and deck 13 with a thickness of 6 mm in contrast to the 5 mm used for them all in Naar's case.

The difference in behaviour could also be attributed to a slightly different meshing technique used for this study, which in the case of this work attempted to focus more on correctly modelling the transitional behaviour of finely refined and coarsely meshed areas with a transitional connecting area. Furthermore, the different mesh sizes Naar compared when searching for the most suitable size were evaluated using axial loading only, which is also worth mentioning. It is also unclear exactly which one of the mesh sizes from the comparison Naar used in his study. Additionally, the objective of that work is primarily the validation of his CB method, by having it include buckling phenomena significant enough to affect the global stiffness of the structure visibly, leading to the findings presented in this present study be overlooked. Another cause might simply be the difference in solver.

Most noteworthy though, is what the results do have in common, namely the fact that both deflection curves follow perfectly linear paths at these levels of loading. The deflection level themselves are less telling, since selecting different points at midship yields different values, and using the exact same points was a challenge as there is no mention of the specific point used in the work by Naar (Naar, 2006). Also, the structural differences would make a quantitative comparison irrelevant.

With regard to the calculated vertical deflection of various points along ship length, the results appear to be both in line with the included qualitative description of the global structural behaviour, and with what was shown by Parmasto's study with a similar ship structure. The major difference being that said case study portrayed the structure under hogging condition, effectively resulting in an exact opposite display of this behaviour. The behaviour of the forces acting on the decks too, is

fully in line with what was observed in Parmasto's work, the only difference being, once again, the sign of the forces as the loading conditions were opposite (Parmasto, 2012). This strengthens the case of the credibility and effectiveness of the method used for the study.

What has clearly emerged however, is that linear analyses are insufficient when it comes to predicting the behaviour of the hull-superstructure interaction and its effects on all the structural components, as they have been shown to incorrectly represent the load sharing mechanisms of the secondary and tertiary structures when elastic buckling occurs. This is a problem, as these findings show that they are closely linked to the hull-superstructure interaction.

The behaviours captured at a local level resemble the load shedding nonlinear behaviour of stiffened deck plates that was observed by both Lillemäe et al. and Palm, according to which, as the deck plate gradually loses stiffness due to elastic buckling, more load is shed to the stiffeners and longitudinal elements such as the girders or bulkheads (Lillemäe et al., 2015; Palm, 2016). Ekman's work also stresses and demonstrates this, while additionally proposing a computationally low-cost modelling solution to address the issue (Ekman, 2020). Furthermore, what the findings underline is that load shedding mechanism are not at all simple and require appropriate investigative methods, especially for complex structures such as those of large passenger ships. An exemplary demonstration of this complexity is the behaviour of the longitudinal girder at deck 5 furthest (1760mm) from the CL, which somewhat counter intuitively appeared to actually carry less load once the deck plates had buckled, as opposed to the longitudinal girder closest to the CL (see Figure 25). Its distance from the origin of where the buckling initiates is most likely the cause, implying that supporting structures closer to this location carry a proportionally far greater share of the load than expected once buckling occurs, while others become more inefficient. Simplistic analyses will not capture minutiae comparable to these. Misunderstanding such phenomena can potentially lead to over dimensioning during the design phase, which in turn heightens overall costs significantly (Guedes Soares, 1987; Guerreiro et al., 2019).

The modelling approach used in this study (meshing and/or solver setting selection) was discovered to be limited with regard to being able to reach levels of buckling and deformations great enough to cause noteworthy changes in global stiffness or in the overall global behaviour of the hull girder. As shown by the nonlinear behaviour exhibited by the longitudinal girder of deck 5 (Figure 25), the Newton-Raphson (N-R) approach is capable of capturing local nonlinearities. However, it faces challenges with levels of nonlinearity which are closer to the limit state, where the tangent stiffness matrix becomes singular, as would be the case if the global stiffness behaviour were to change significantly. When approaching load levels capable of causing significant behavioural changes, the simulation exceeds the number of allowed iterations, which when raised, would be unable to converge, especially when supposedly more efficient nonlinear solver algorithms such as the Modified N-R were attempted. These resulted in extremely long computation time caused by convergence issues, which would finally exceed available memory capacity. These issues were exacerbated when trying to use the Arc-length method. This indicates that those methods, which are designed to shorten computational time, are best suited for studies involving simulations of geometries which are simpler and/or exhibit less drastic changes in structural behaviour. They would perhaps have proven viable for this study too, had the computational resources available been far greater.

This finding indicates that FEMAP's nonlinear solver might not be the most appropriate tool for this type of study, at least without greatly reducing the number of elements though appropriate

geometry idealization strategies such as laminate elements. Naar's model, which was solved using LS-DYNA and was meshed following a similar strategy to the one used for this study, was capable going far beyond the load levels achieved here (Naar, 2006).

Finding the most appropriate nonlinear solver settings for FEMAP to greatly reduce the computational complexity and allow this method to be employed and in the future take advantage of its full potential, would be a great subject worthy of further study. Another way to move forward in the attempt to properly capture elastic buckling, the resulting load shedding and its effect on the global level, would be to expand the panel based linear method developed by Palm or integrate laminate elements such as that developed by Ekman (Palm, 2016; Ekman, 2020). These methods, which until now has only been proven to work with a satisfying degree of effectiveness for individual decks or simplified box girder structures, have great potential for allowing these phenomena to be studied accurately while requiring a commercially reasonable amount resources, in terms of time and required computational capacity.

6. Conclusion

This thesis attempted to model the effects of elastic buckling at sub critical loads in a modern passenger vessel, while assessing consequential changes in global and local behaviour. The method consisted of subjecting said structure to a sagging loading condition and creating a strategically locally refined mesh, capable of providing a highly accurate representation of the structure's behavioural mechanisms and to compare the nonlinear analyses results with those obtained using a traditional linear approach. Four-noded quadrangular and three-noded triangular 3D elements make up the arrangement use for modelling the plates. Primary stiffeners were modelled using four-noded quadrangular S4 elements for both web and flange. In the areas of the vessel with a relatively fine mesh, the density and location of which being selected based on the results of successful relevant past studies conducted by other authors, the offset beam technique was used to model stiffeners. The stiffener webs modelled with shell elements and flanges as beam elements. At coarse areas of the structures, beam elements were used for secondary and tertiary structures, with rigid body elements used in the transition zone between fine and coarse mesh zones, to ensure the stiffener webs would maintain realistic behaviour when connected to the beam elements. Pillars were modelled using representative beam elements along the entire ship length.

On a global scale and at the load levels studied, no major effect on the overall stiffness of the vessel was found. However, there is strong reason to believe this would not be the case if the structure were subjected to loads high enough to cause more decks to buckle. The effects would be especially significant if the shell of the recess area subjected to shear connecting hull and superstructure were to buckle at x=3L/4. On a more local level, it was shown that there are significant differences between the loads calculated to be acting on each of deck. It was shown that at the onset of elastic buckling, the loss of stiffness in the deck plates results in an increase of load bearing efficiency of primary stiffeners such as longitudinal girders, especially areas in close proximity to where the buckling first occurs. The classic linear method is incapable of correctly representing the load shedding phenomena that occur at the secondary and tertiary hierarchical levels when elastic buckling does occur. This leads to misunderstanding the load carrying mechanisms which in turn can result in costly erroneous design assumptions resulting in costly over dimensioning. These findings can be expanded in future work, by reaching load levels capable of altering the overall global behaviour of the structure and mapping all the areas of the vessel where elastic buckling is prone to occur, while quantifying the potential saving by improving design choices through the use of methodology presented in this thesis.

References

Andric, J. & Zanic, V. 2010. The Global Structural Response Model for Multi-Deck Ships in Concept Design Stage. Ocean Engineering, Vol. 37, pp.688-704.

Avi, E. et al. 2015. Equivalent shell element for ship structural design. Master's thesis. Aalto University School of Engineering, Department of mechanical Engineering, Ship Laboratory. Espoo. 62 p.

Benson S., Downes J., Dow R.S., 2014. Overall buckling of lightweight stiffened panels using an adapted orthotropic plate method. Engineering Structures 85 (2015) 107–117.

Bleich, H.H. 1952. Nonlinear Distribution of Bending Stresses due to Distortion of the Cross Section. J. Applied Mechanics. vol. 29. p. 95-104.

Caldwell, J. B. 1957. The effect of superstructures on the longitudinal strength of ships. The Institution of Naval Architects. Vol. 99, p. 664.

Caldwell, J. B. 1965. Ultimate Longitudinal Strength. The Institution of Naval Architects. Vol. 107.

Cook R. D., Concepts and Applications of Finite Element Analysis. New York: Wiley, 2001. ISBN 978-0-471-35605-9.

Cruise market watch, 2020. Increase in cruise ship passengers carried prior to the 2020 pandemic. https://cruisemarketwatch.com/growth/, 2021.

DNVGL, 2015. Buckling Class Guideline. DNVGL-CG-0128.

DNVGL, 2015*. Buckling Class Guideline. Pt. 3 Ch.1 Sec. 14. DNVGL-CG-0128.

DNVGL, 2016. Finite Element Analysis. DNVGL-CG-0127.

DNVGL, 2018. Direct Strength Analysis of Hull Structures in Passenger Ships. DNVGL-CG-0138.

DNVGL, 2018*. Wave loads - Rules and standards. DNVGL-CG-0130.

Ehlers, S. 2011. Large Complex Structures. Lecture Notes (2nd version). Aalto University School of Engineering, Department of Mechanical Engineering, Ship Laboratory. Espoo.

Ekman, E. 2020. Development of simplified nonlinear response analysis procedure for ship structures. Department of Applied Mechanics. Naval Architecture. Aalto University, Espoo.

Engineering, Department of mechanical Engineering, Ship Laboratory. Espoo.

Gannon L., Liu Y., Pegg N., Smith M. J., 2012. Effect of welding-induced residual stress and distortion on ship hull girder ultimate strength. Marine Structures 28 (2012), 25-49.

Guedes Soares, C. & Gordo, J., 1997. Design methods for stiffened plates under predominantly uniaxial compression. Marine Structures, Volume 10, p. 465–97.

Guedes Soares, C. & Soreide, T. H., 1983. Behavior and design of stiffened plates under predominantly compressive loads. International Shipbuilding Progress, Volume 30.

Guerreiro J., Martins R., Batistac R.F.P, 2019. Structural resistance of lightweight stiffened panels submitted to buckling. First International Symposium on Risk and Safety of Complex Structures and Components.

Heder M, Ulfvarson A. Hull beam behaviour of passenger ships. Marine Structures 1991; Vol 4(1). p. 17-34.

ISSC, 1997. Proceedings of the 13th International Ship and Offshore Structures Congress. Trondheim

Kim, N., 2014. Introduction to nonlinear finite element analysis. New York: Springer.

Kujala, P. 2003. Development of Innovative Structural Concepts for advanced Passenger Vessels.

Lillemäe et al., 2013. Influence of initial distortion on the structural stress in 3 mm thick stiffened panels. Thin-Walled Structures 72 (2013), 121-127.

Lillemäe et al., 2014. Influence of initial distortion of 3 mm thin superstructure decks on hull girder response for fatigue assessment. Marine Structures vol 37(2014). 203–218.

Melk, K. 2011. Shear-Induced Secondary Bending Response at Balcony Opening of Passenger Ship. Master Thesis. Aalto University, Department of Applied Mechanics, Espoo.

Muckle, W. 1962. The influence of Large Side Openings on the Efficiency of Superstructures. Trans. RINA, p.177-178.

Naar H. et al. 2004. A Theory of Coupled Beams for Strength Assessment of Passenger Ships. Marine Structures 12. vol 17(8). pp. 590-611.

Naar H., 2006. Ultimate Strength of Hull Girder for Passenger Ships. Doctoral Dissertation. Helsinki University of Technology, Department of Mechanical Engineering, Ship Laboratory. Espoo, 2006.

NAFEMS, 1992. Introduction to Nonlinear Finite Element Analysis. s.l.:NAFEMS Ltd..

Palm A.M., 2016. Buckling and Load Shedding in Redundant Plated Ship Structures. Master Thesis. Department of Marine Technology. Norwegian University of Science and Technology.

Parmasto, O. 2012. Mechanics of the passenger ship structure with non-longitudinal-load-carrying accommodation decks. Department of Applied Mechanics. Naval Architecture. Aalto University, Espoo.

Paik, J. K. & Kim, B. J., 2002. Ultimate strength formulations for stiffened panels under Combined axial load, in-plane bending and lateral pressure: a Benchmark study. Thin-Walled Structures, Volume 40, p. 45–83.

Raikunen, J. 2015. Optimization approach for passenger ship structures using Finite Element Method. Aalto University School of Engineering, Department of mechanical Engineering, Ship Laboratory. Espoo, 2015.

Raikunen J., Avi E., Remes H., Romanoff J., Lillemäe-Avi I. & Niemelä A. (2019): Optimisation of passenger ship structures in concept design stage, Ships and Offshore Structures, DOI: 10.1080/17445302.2019.1590947

Reddy, JN. 2004. Introduction to Nonlinear Finite Element Analysis. Oxford University Press, Incorporated. EBook ISBN 9780191574672. Aaalto E-Library.

Reddy*, JN. 2004. Mechanics of laminated composite plates and shells – theory and analysis, 2nd ed. Boca Raton (FL): CRC Press.

Remes, H. et al. 2011. Hull/Superstructure-interaction in optimized passenger ships. Advances in Marine Structures. p. 625-632.

RIKS, E., 1979. An incremental approach to the solution of snapping and buckling problems. International Journal of Solids and Structures, 15(7), pp. 529-551.

Romanoff J., Remes H., Varsta P., Jelovica J., Klanac A., Niemelä A., Bralic S. & Naar H. (2013) Hull-superstructure interaction in optimised passenger ships, Ships and Offshore Structures, 8:6, 612-620, DOI: 10.1080/17445302.2012.675196

Romanoff, J. et al. 2011. Interaction between web-core sandwich deck and hull girder of passenger ship. Aalto University, Espoo.

Romanoff, J et al. 2016. Influence of Nonsymmetric Steel Sandwich Panel Joints on Response and Fatigue Strength of Passenger Ship Deck Structures. Journal of Ship Production and Design, Vol. 32, No.3, August 2016, pp. 1-9.

Romanoff, J., Karttunen, A.T., Varsta, P., Remes, H. and Reinaldo Goncalves, B., 2020. A review on non-classical continuum mechanics with applications in marine engineering. Mechanics of Advanced Materials and Structures, ahead-of-print(ahead-of-print), pp. 1-11.

SIEMENS, 2019. Simcenter Nastran Handbook of Nonlinear Analysis.

Smith, C.S. 1975. Compressive Strength of Welded Steel Ship Grillages. US Defence Research Information Centre, AD-A023670, May 1975.

Smith, C.S. 1977. Influence of Local Compressive Failure on Ultimate Longitudinal Strength of a Ship's Hull. PRADS International Symposium on Practical Design in Shipbuilding. Tokyo, Oct. 1977.

Steen, E., Byklum, E. and Hellesland, J., 2008. Elastic post buckling stiffness of biaxially compressed rectangular plates. Engineering Structures, 30(10), pp. 2631-2643.

STX/Mayer Turku, 2018. Increase in passenger vessel size. Principles of naval architecture course slides, Aalto University. Espoo, 2018.

Vasta, J. 1949. Structural Tests on the Passenger Ship S.S. President Wilson – Interaction between Superstructure and Main Hull Girder. Trans. of the society of Naval Architects and Marine Engineers. vol.57, p.253.

Zienkiewicz, O.C. 1971. The Finite Element in Engineering Science. USA: McGraw Hill.

Appendix 1

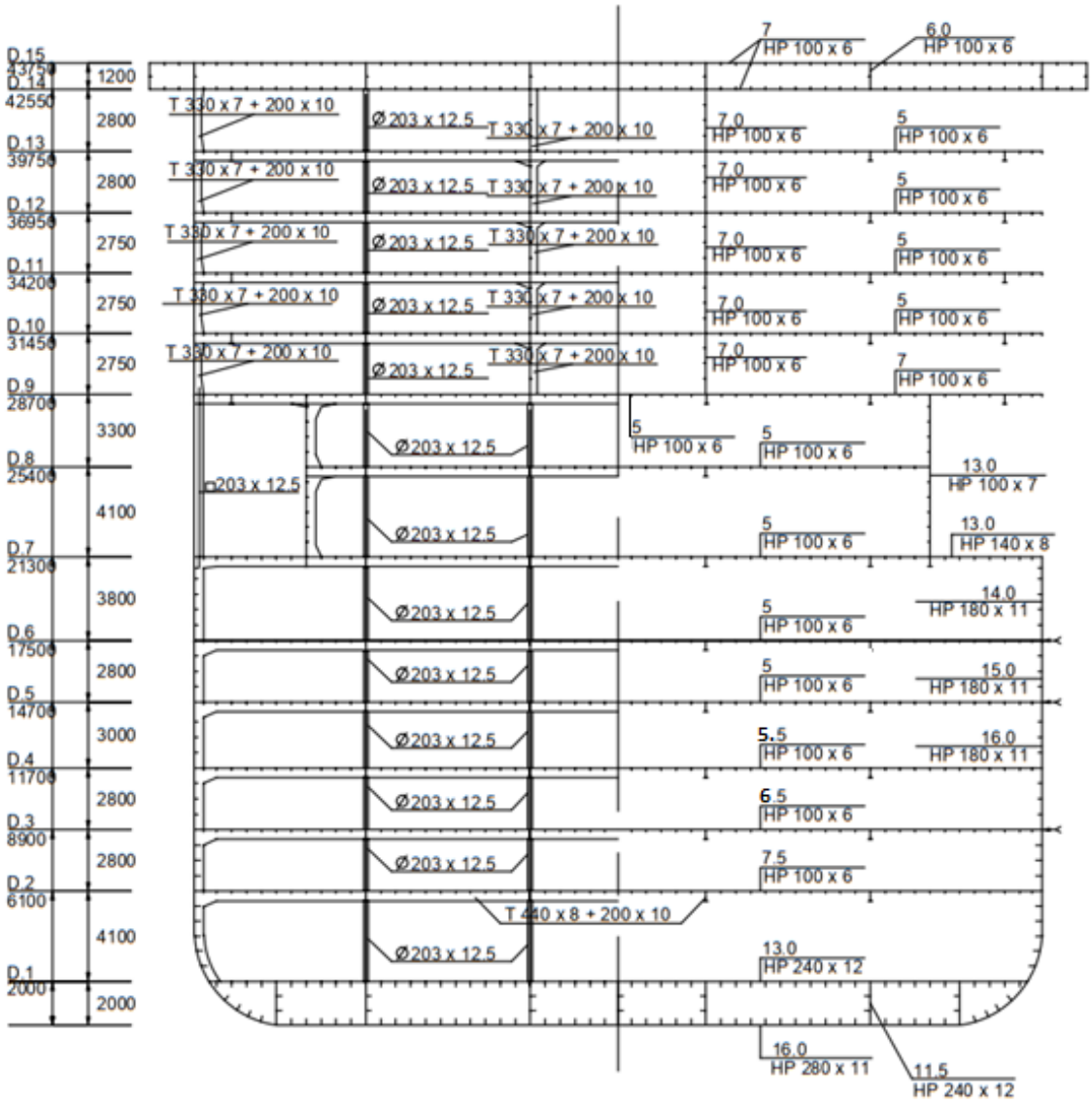

FRAME SPACING (GENERALLY)	680 mm
WEB FRAME SPACING (GENERALLY)	2730 mm
PILLAR SPACING (GENERALLY)	2730 mm

Based on:		Aalto University School of Engineering	
Part of:			
Replaces:			
Designer: Alexander Jerne Date: 03.06.2020		Title: Appendix 1. The main frame	
Checked by.: Date:			
Approved by: Date:			
Program: AutoCAD 2010	Paper size A4 (210x297)	Drawing number:	Rev.
Mass:	Scale: 1:300		Page 1 (pages) (1)